STUDY OF A COPOLYMER FOR CERAMIC PROCESSING

BY

YAN YANG

A THESIS
SUBMITTED TO THE FACULTY OF

ALFRED UNIVERSITY

IN PARTIAL FULFILLMENT OF THE REQUIREMENTS
FOR THE DEGREE OF

MASTER OF SCIENCE
IN
MATERIALS SCIENCE AND ENGINEERING

ALFRED, NEW YORK

MAY, 2015

STUDY OF A COPOLYMER FOR CERAMIC PROCESSING

BY

YAN YANG

B.S. ANHUI UNIVERSITY OF SCIENCE AND TECHNOLOGY (2008)

SIGNATURE OF AUTHOR_____

APPROVED BY_____
YIQUAN WU, ADVISOR

_____
WILLIAM W CARTY, ADVISORY COMMITTEE

_____
DAVID W LIPKE, ADVISORY COMMITTEE

_____
CHAIR, ORAL THESIS DEFENSE

ACCEPTED BY_____
DOREEN D. EDWARDS, DEAN
KAZUO INAMORI SCHOOL OF ENGINEERING

ACKNOWLEDGMENTS

First of all, I would like to express my sincere and deepest gratitude to my advisor, Dr. Yiquan Wu, for his guidance, advice and support through all the study and life in Alfred University. Thanks for his patience, diligence, and motivation, which encourage me to be a more independent-thinking student and do a better job on the research work.

I am very thankful to Dr. William W Carty and Dr. David W Lipke for their valuable guidance on my thesis work. Their help on my research gives me a better understanding on the mechanisms of the research, and supply me better methods to solve the experimental challenge.

Additionally, I must acknowledge Hyojin Lee, Gerald L Wynick, Francis A. Williams, Mirela Dragan, Swavek Zdzieszynski, and Timothy Keenan for their help with all of the characterization of my research work. I also would like to thank all other technical specialists for their help with training the instrument and equipment that were essential to my success.

I am very thankful to Panadyne Inc. for supplying Al_2O_3 powders, and Kuraray America Inc. for donating the organics.

I would like to thanks the colleagues: Yiyu Li, Yin Liu, Sureporn Chortirawit for their help in my work and life. Especially, I want to express my thanks to Katie Decker and Anatoly Kishinevski for his help with thesis paper review.

I also want to express my thanks to Professor Shunzo Shimai for his inspiration and suggestion about my research work.

Finally, thanks to my family for all of their encouragement at the most important time, I could not complete my degree without their support.

TABLE OF CONTENTS

Page

LIST OF TABLES

Page

LIST OF FIGURES

Page

ABSTRACT

A copolymer of isobutylene and maleic anhydride (IB-MA) is a new environmentally friendly and multifunctional organic, which can work as a dispersant, a spontaneously gelling agent, and a binder for aqueous casting process. IB-MA was applied to aqueous gelcasting and tape casting techniques for ceramics production.

Environmentally friendly IB-MA can work as both a dispersant and a spontaneously gelling agent for ceramic aqueous processing, which can shorten the ceramic production time, lower the cost, and green to the environment. For the gelcasting process, alumina (Al_2O_3) powder was chosen as the raw ceramic materials. The morphology of the ceramic powders was measured. The rheological properties of ceramic slurries were investigated as a function of solid loading and IB-MA concentration. Al_2O_3 ceramic green bodies with large size and complex shapes were successfully produced by the IB-MA spontaneous gelling system. The microstructures of Al_2O_3 ceramic in different processing stages were observed by the scanning electron microscope (SEM). Translucent Al_2O_3 ceramics were obtained after the de-binding and final vacuum sintering process.

Meanwhile, environmentally friendly IB-MA can work as both a dispersant and a binder for ceramic aqueous tape casting, which can simplify the production process, reduce the production cost, and be green to the environment. For the tape casting process, alumina (Al_2O_3) and yttrium aluminate garnet (YAG) powders were used as the raw ceramic materials. The ceramic particle morphology and microstructure of ceramic tapes before and after sintering were investigated by SEM. The rheological properties of the ceramic suspensions were characterized by the viscosity of the systems as a function of shear rate. The optical properties of the obtained vacuum-sintered ceramic wafers were examined in the ultra violet & visible (UV-VIS) and infrared (IR) region. Good quality transparent ceramic wafers were produced by IM-BA aqueous tape casting process.

INTRODUCTION

Ceramic forming techniques include uniaxial dry pressing methods,[1] plastic forming techniques (jiggering,[2] extrusion,[3] injection molding,[4] and 3-D printing[5]), and casting process (slip casting,[6,7] tape casting,[8] and gelcasting[9]). Gelcasting has significant advantages over other processing methods, including: dimensional accuracy, complex shaping, homogeneous structure, simplicity, minimized postsintering machining operations, and decreased manufacturing cost. Recently, more and more flat, thin and large scale ceramics are applied to the fabrication of substrates, packaging and multilayer technology[10-12] (capacitors,[13] sensors,[14] piezoactuator,[15] laser composites,[16] etc.). Tape casting technique is preferred processing to produce flat ceramic wafers with thicknesses ranging from a few microns to a few millimeters by tape casting techniques.

Powder is an important ingredient for batch formulation in the ceramic casting process. The characterization of the starting ceramic powders is essential to decide the category and addition of the dispersant or other organic additives. Important parameters to monitor in powders include average particle size and distribution, specific surface area, and the trace impurity levels. Particle size distribution has an effect on the packing density of ceramic green bodies. Good control of particle size, shape, and distribution can improve green bulk density. Smaller particles have higher specific surface area and surface energy, which can easily form the soft agglomerates. The soft agglomerates can be broken down by the ultrasonic or milling procedure. Soluble impurity contained in the ceramic powders can also change the dispersion behavior of ceramic particles in suspensions.[17,18]

Homogeneous ceramic suspension preparation is very important in ceramic casting process. Mixing is adopted to break agglomerates in the ceramic slurry to improve the chemical and physical uniformity of different components in the ceramic suspension to the microscale. By using dispersants, ceramic particles can be stabilized in the liquid medium by steric stabilization,[13] electrostatic stabilization,[19,20] or electrosteric stabilization.[20] Organics are also needed for different casting process. For gelcasting techniques, gelling agents is critical organic additive, which can be polymerized to form a

strong and cross-linked 3-Dimentional network by adding the initiator to the ceramic slurry. Meanwhile, binders and plasticizers are important organic additives for tape casting procedure. Binders build organic bridges between ceramic particles. After evaporation of the solvent, binders can make ceramic green tapes to be easily manipulated and retained in the desired shapes before sintering. The properties of ideal binder system for ceramic processing includes: providing strength to the green body; enhancing formability; providing lubrication; minimize contamination; non-toxic; and, inexpensive. Binders can change the flow properties, increase the mean viscosity of the suspensions, and effectively thicken the system. With high-viscosity suspension, flocculation can improve the suspension consistency to be like a paste and slow down the particle sedimentation.

Rheological property of a suspension is important for the tape casting process. The apparent viscosity (Pa•s) varying with shear rate (s^{-1}) is recorded to evaluate the rheological property of the ceramic suspension. Rheology is controlled by five factors:[21]

- Particle-particle interaction;
- Particle size and distribution;
- Particle morphology;
- Particle concentration (water content);
- Rheology of the suspension medium.

Viscosity of the ceramic suspension needs to be adjusted in different casting processes. Ceramic suspension with low viscosity is demanded for degassing and fast fluid flow behavior in the slip casting process. However, enough viscosity is required to improve the friction between ceramic suspension and Mylar carrier to keep the desired shapes.

Investigation on the microstructure of ceramic green body can supply the information about the homogeneity of different components in ceramic casting and sintering process. Homogeneous distribution of ceramic particles in the green bodies can benefit for the uniform shrinkages of the ceramics in the drying and sintering process with less cracks, wrapping and other defects.

LITERATURE REVIEW

A. Gelcasting processing for ceramic fabrication.

Gelcasting was first developed at Oak Ridge National Laboratory,[22-24] and attracted more research on the ceramic fabrication by the gelcasting technique. Gelcasting is a simple, near-net shaping, and convenient technique to produce ceramic parts with the regular and complex shapes. In gelcasting techniques, ceramic powders and monomer solutions are mixed homogeneously to form a slurry with high solids loading and low viscosity. The slurry is poured into a mold and polymerization begins with or without the addition of a chemical initiator. Over a period of time, polymer gel networks are formed *in situ* to the shape of the mold. During the polymerization, all the ceramic particles are stabilized in the cross-linked gel network. The ceramic green bodies are removed from the mold for drying. After burning out the organic additives, the ceramic parts are obtained after the final sintering stage.

The development of gelcasting techniques has experienced four major periods:

(1) Free-radical polymerization gelling system

The flow chart for free-radical gelcasting procedure is shown in Figure 1. Acrylamide polymer methacrylamide (MAM)[24] was used to get the high solids loading and low viscosity ceramic suspension to produce good quality alumina with complex shapes. Poly (vinyl alcohol) (PVA)[25] was used as the monomer coupling with an organotitanate for the gelcasting formation of alumina green bodies, which reaction can be influenced by the cross-linking agent concentration, temperature and solid volume fraction. However, the presence of oxygen can prematurely terminate the polymerization reaction by forming a peroxide group at the end of the polymer chain, which is solved by using an inert atmosphere to avoid the interference of oxygen.

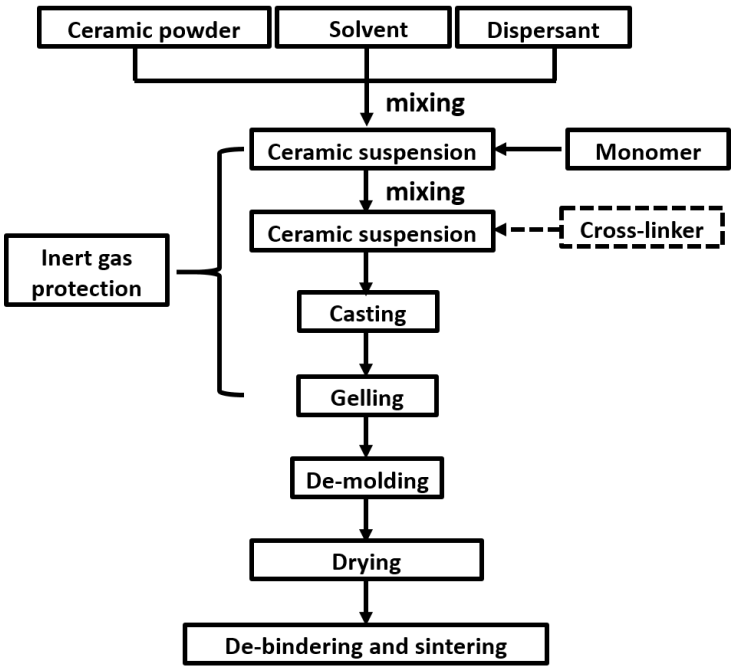

Figure 1. Flow cart for free-radical gelcasting techniques.

(2) Surrounding-triggered gelling system (including thermo-reversible gelcasting)

Ceramic fabrication using surrounding-triggered gelling system is described in Figure 2. Acrylic systems with poly (methyl methacrylate) (PMMA) end-blocks and a poly (n-butyl acrylate) (PtBA) mid-block is an example of ABA-type triblock copolymers with the midblock selectively dissolved in the solvent and aggregated end blocks linked by the well-solvated mid-blocks to form physical gels. Acrylic system can gel in ethanol to produce alumina ceramic green bodies,[26] schematically shown in Figure 3. Water soluble polysaccharides, such as agarose, can gel in water during the heating process to produce zirconia ceramic parts with sufficient wet green body strength.[27] Photo-polymerization can solidified with UV light by transport of photons in the suspension to produce silica with complex shapes.[28] Surrounding-triggered gelling systems can be operated in air atmosphere. However, the viscosity of the suspension is high with the end-blocks reactions driven by the temperature, solvent, or light illumination.

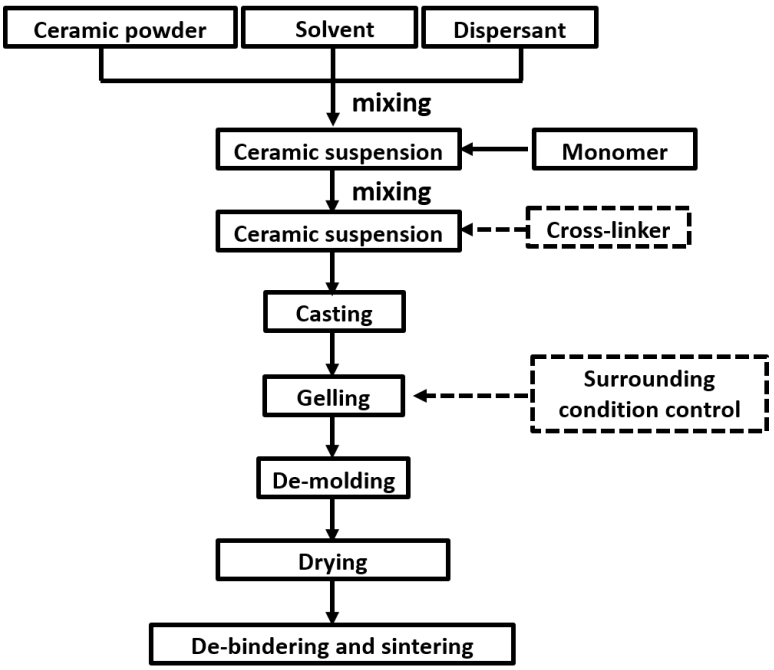

Figure 2. Flow chart for surrounding-triggered gelcasting procedure.

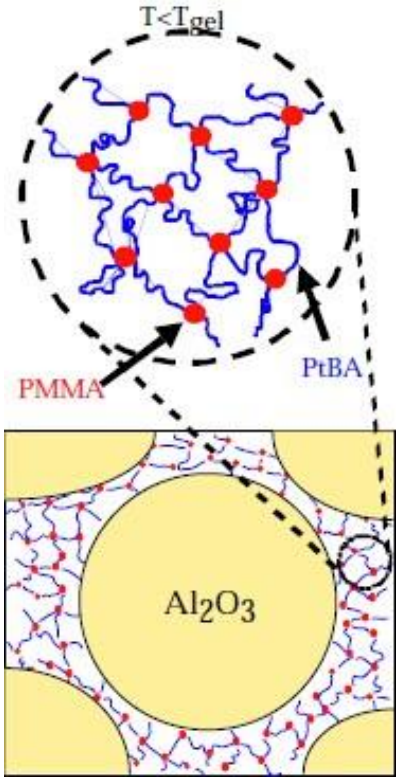

Figure 3. Schematic illustration of thermal-reversible gelling agent with network formation in ceramic suspension.[26]

(3) Nucleophilic addition reaction gelling system.

Takeshita and Kurita[29] reported the gel formation of yttria-partially stabilized zirconia (Y-PSZ) ceramics in air with three kinds of additives, which is caused by the nucleophilic polymerization between epoxy resin and amine. This gelling system is low toxicity, and absence of oxygen inhibition. More researchers are inspired to devote efforts on researching nucleophilic polymerization in the gelcasting techniques. The nucleophilic polymerization between epoxy resin and hardener can be conducted at room temperature in aqueous[30] or non-aqueous media[31] in the air atmosphere to produce dense ceramics, translucent ceramics and porous ceramics.[32] However, the dispersant, monomer and cross-linker are still toxic, which threaten the operator and the environment. The toxicity of the nucleophilic polymerization encourages more research on developing new organic additives with lower toxicity.

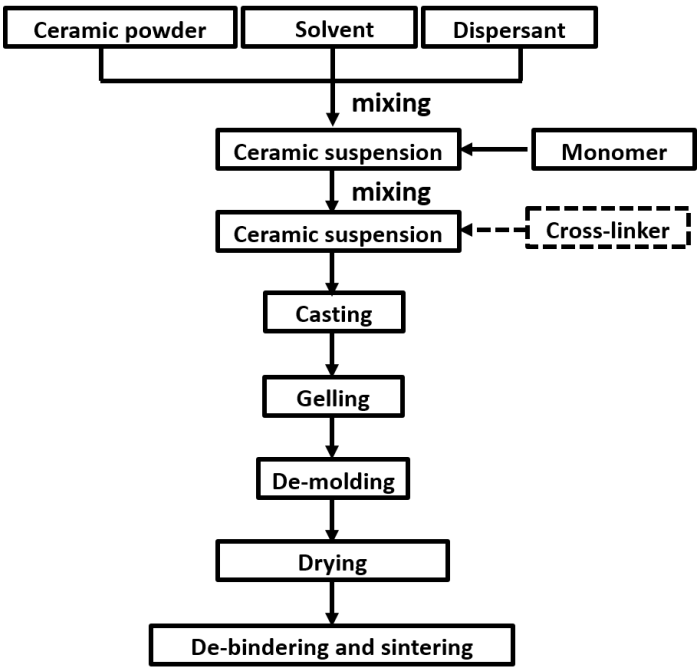

Figure 4. Flow chart for nucleophilic polymerization gelcasting procedure.

(4) Spontaneous monomer gelling system

Spontaneous gelling additive is desirable for the gelcasting system, which can simplify ceramic processing, shorten the operation time, and lower the cost for the production, shown in Figure 5. A multifunctional organic, poly (isobutylene-alt-maleic anhydride) (IB-MA) was explored with the structural formula shown in Figure 6. IB-MA can work as a dispersant for ceramic powders, which can spontaneously form gels at room temperature without special control on the temperature and atmosphere, shown in Figure 7. IB-MA has been used to produce dense ceramics,[33] porous ceramics,[34] and transparent ceramics[35] with regular shapes. Polyurethane (water-proof painting to prevent hydrolysis) coated AlN[36] and yttria (Y_2O_3)[37] can also be produced using IB-MA as the dispersant and spontaneously gelling agent.

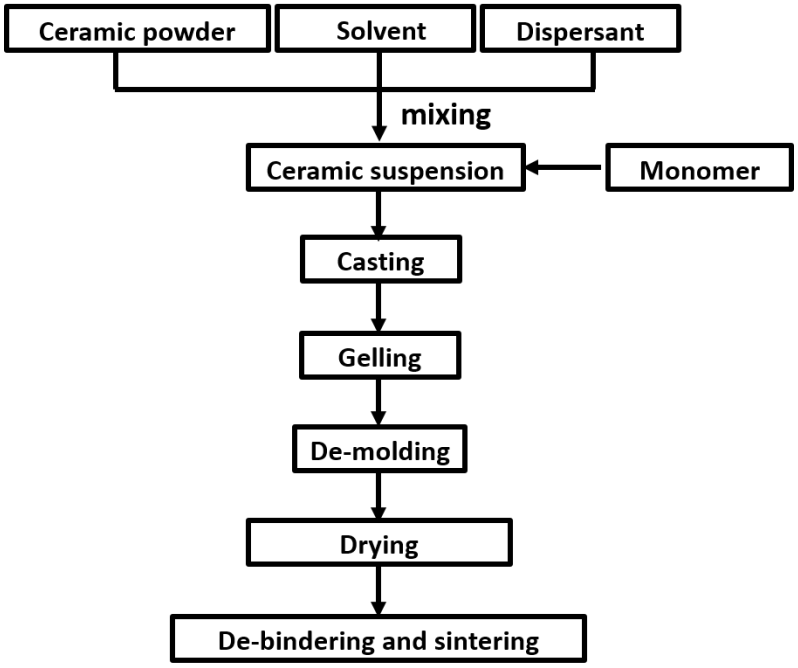

Figure 5. Flow chart of spontaneous gelling system for ceramic fabrication.

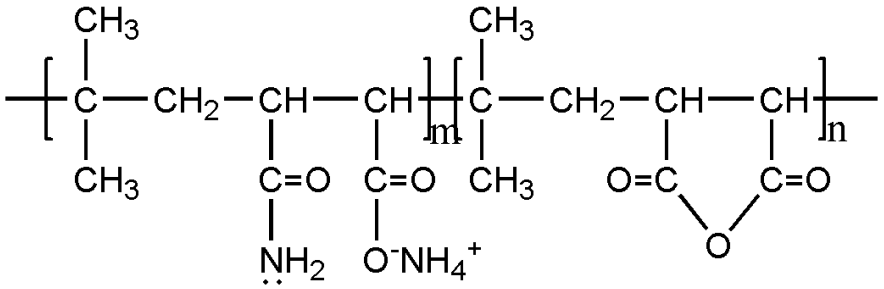

Figure 6. Chemical formula of IB-MA.

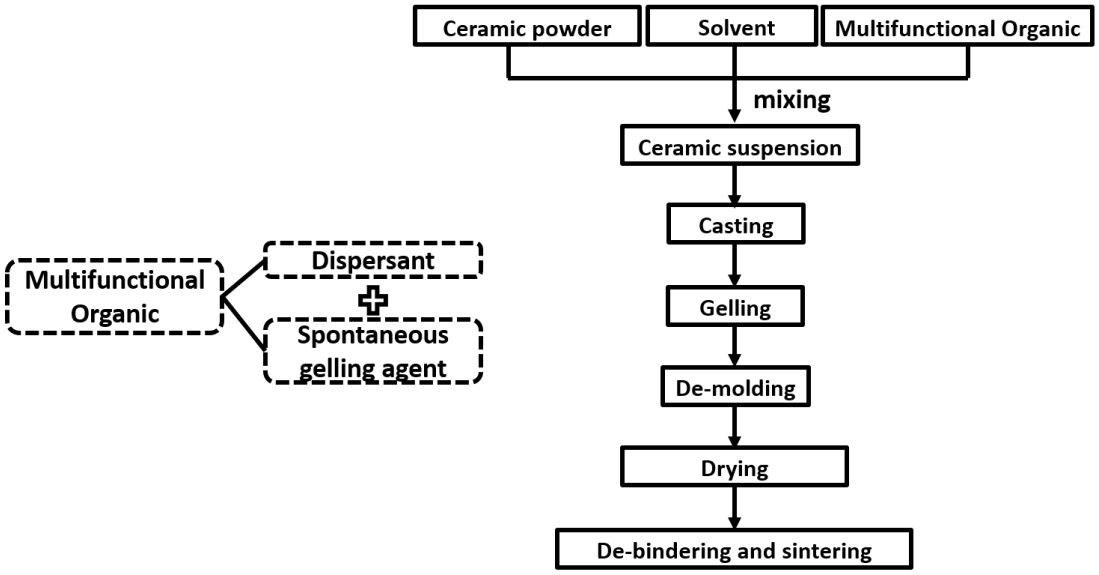

Figure 7. Flow chart of spontaneous gelling system using a multifunctional organic for ceramic processing.

Another similar multifunctional copolymer of poly (isobutylene-alt-maleic anhydride) 600AF (IB-MA 600AF), was recently researched to estimate the dispersion ability and the spontaneous gelling function. The structural formula is presented in Figure 8. Alumina (Al_2O_3)[38] ceramic suspension with solid loading as high as 46vol% were made using organic mixture of IB-MA 600AF and IB-MA, indicating the potential application of IB-MA 600AF on the ceramic casting techniques.

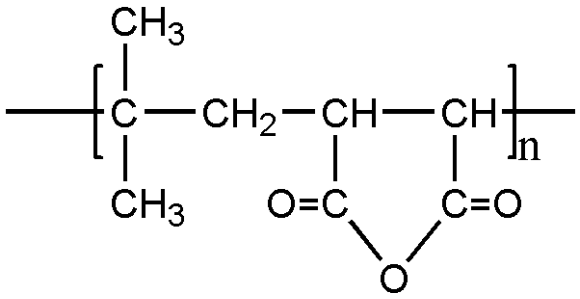

Figure 8. Chemical structural of IB-MA 600.

B. Tape casting procedure for ceramic wafer production.

Tape casting techniques have a major impact on a myriad of practical applications in the ceramic sheet production, such as multilayer ceramic packaging,[39] multilayer capacitors,[40] electronic substrates,[41] solid oxide fuel cells,[42] and laminated composites for structural materials.[43] The thin, flat ceramics can also be patterned, stacked and laminated to form three-dimensional structures.

Since Howatt first used tape casting to prepare ceramics in 1947,[44] tape casting technique, also known as the doctor blade process, has been widely used for ceramic production, shown in Figure 9. The flow chart for the ceramic tape casting is depicted in Figure 10. The ingredients for tape casting includes ceramic powders, solvent, dispersant, binder, and plasticizer, which are mixed together and then made to flow under a moving (or static) blade on the static (or moving) plastic substrate. The thickness of the slurry is controlled by the height of the doctor blade gap and the moving speed between the blade and substrate.

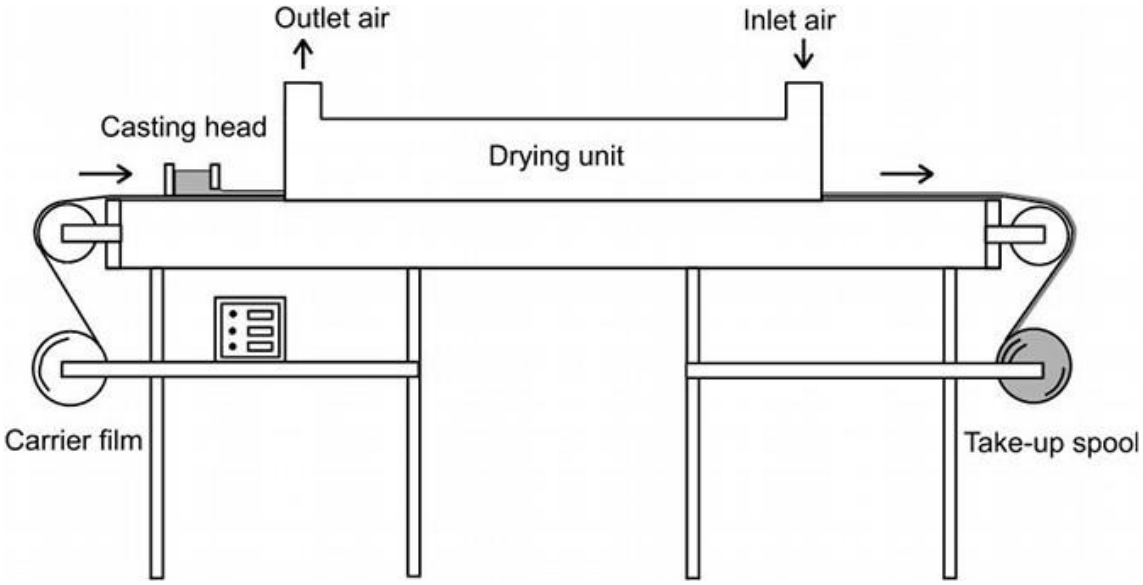

Figure 9. Schematic diagram for the ceramic slurry tape casting.

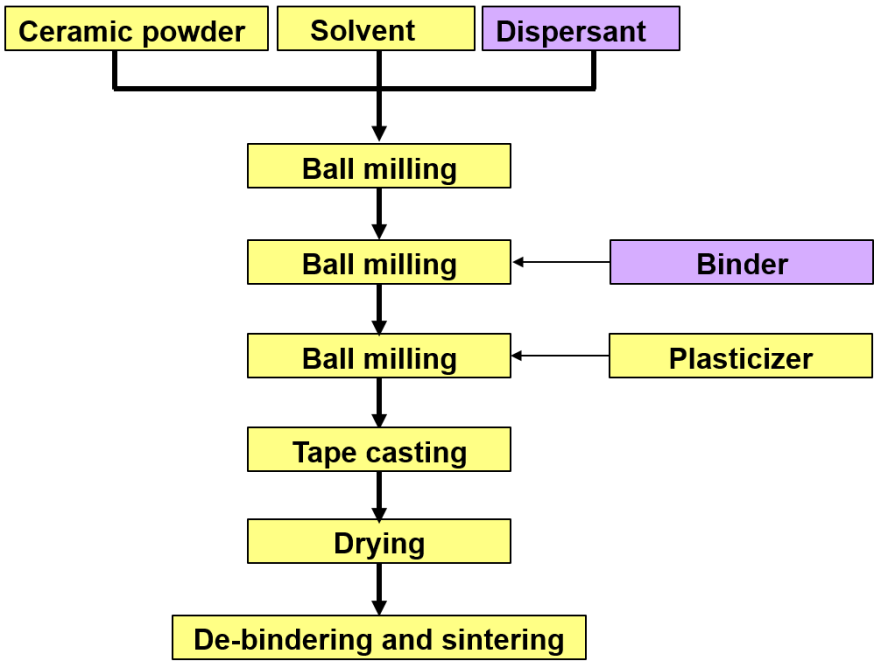

Figure 10. Flow chart of tape casting for ceramic tape fabrication.

The systems for tape casting mainly include two categories: non-aqueous[11,16,45-48] and aqueous tape casting.[7,49-54] Non-aqueous tape casting systems adopt organic solvents, making use of their properties of non-hydration with ceramic powders, good wetting behaviors, and easy drying process. However, special protections are needed because of the flammability, toxicity, volatility, which cause high cost for the production. As a result, increasing attentions are paid to aqueous tape casting, which can make up most of the disadvantages of non-aqueous systems except for the slow evaporation process.

Binders are polymers that are adsorbed and bridged between ceramic particles to provide the interparticle flocculation and the bonding action. Binder is an important additive for the tape casting system. The ceramic green tapes are obtained by impregnating the polymer matrix (binder) with large amounts of ceramic materials. Binders can influence the green tape properties (strength, flexibility, durability, toughness and smoothness, etc.).[55]

For aqueous tape casting, the criteria for developing binders mainly include:[56] (1) stability; (2) appropriate viscosity of a powder suspension; (3) sufficient green strength of the as-dried products. Binders can build organic bridges between ceramic particles. After evaporation of the solvent, binders can make ceramic green tapes to be easily manipulated and retained in the desired shapes before sintering.

Recently, water-soluble binders developed for aqueous tape casting to produce thin ceramic tapes, include derivate of cellulose ethers,[41] Polyvinyl alcohols (PVA),[52,57] acrylic polymers,[58] and acrylic polymer emulsions.[49,59] D. Hotza summarized the research on the aqueous tape casting of alumina and mullite in Table I.[50]

Table I. Aqueous Slurry Additive for Tape Casting of Alumina and Mullite[50]

Powder	Binder	Plasticizer	Dispersant	Ref.
Al_2O_3+MgO	Acrylic polymer	PEG+BBP	Condensed aryl sulfonic acid	60
Al_2O_3+talc	PAA	Glycerol	NH_4PMA+Dispex A40	61
	PAA	Glycerol+PVP	NH_4PM+Dispex A40	
Al_2O_3	PUR		POENPE	62
	PVA	Glycerol	POENPE	
	PVAc	Glycerol	POENPE	
	NH_4PA	Glycerol+DBP	Primal 850	
Al_2O_3	Cellulose ether		NH_4PMA	63
Al_2O_3	Acrylic copolymer	BBP	NH4 salt of a polyectrolyte	64
Al_2O_3	Acrylic polymer	PPG	NH_4PMA	65
Mullite	Acrylic polymer	PPG	NH_4PMA	66
Al_2O_3	HEC	PEG	NH_4PA	49
Al_2O_3	AE/AA			67
	AE/AA		Acrylic dispersants	68
Al_2O_3	PAA	PEG	NH_4PA	69

Interestingly, Reddy et al. reported the dispersant effect of binders in tape cast slurries,[70] which indicated the possibility of simplifying the tape casting process by removing the necessity of dispersant. IB-MA has been recently reported as a spontaneous gelling agent and an effective dispersant in aqueous systems, [33-35,37,38,71] which has the promising application as a binder for ceramic tape casting techniques. IB-MA can work as a dispersant for Al_2O_3 powder to change the isoelectric point (IEP) from pH=8.3 to pH=5.8 with the addition of IB-MA 0.3wt% (powder weight based).[33] IB-MA can also change the IEP point of polyurethane coated AlN from pH= 7.8 to pH = 3.5 with ζ-potential increase from 0mV to -40mV.[36] The good dispersion ability of IB-MA indicates the good adsorption of IB-MA to the ceramic particle surface. The function of IB-MA as

a binder and a dispersant for ceramic powder can efficiently simplify the production procedure (Figure 11), and lower the cost for the equipment.

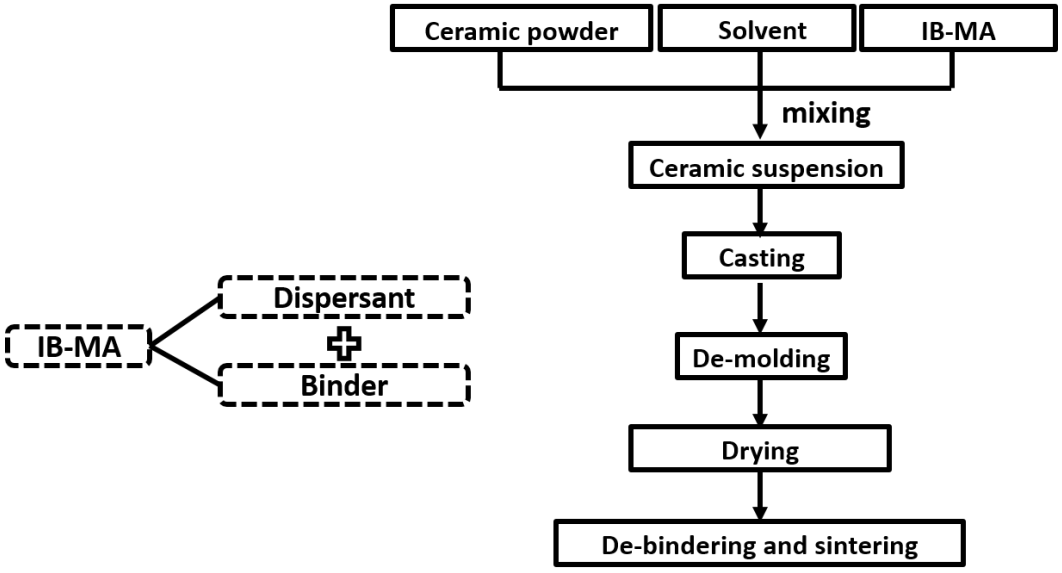

Figure 11. Flow chart of tape casting for ceramic tape fabrication using IB-MA.

Meanwhile, plasticizers are also needed to increase the flexibility of ceramic green tape by changing the glass transition temperature (T_g). Commonly used plasticizers are listed in Table II. Ethylene glycol is effective in lowering the glass transition temperature of binder.[72] The plasticizing action of ethylene glycol decreases as its molecular weight increases. A plasticizer with a relative high boiling point is also important to ensure the system stable at elevated temperature.

Table II. Commonly Used Plasticizer

Plasticizer	Melting point(°C)	Boiling point(°C)	M.W.(g/mol)
Water	0	100	18
Ethylene Glycol	-13	197	62
Diethylene glycol	-8	245	106
Triethylene glycol	-7	288	150
Tetraethylene glycol	-5	327	194
Polyethylene glycol	-10	>330	300
Glycerol	18	290	92
Dibutyl phthalate		340	278
Dimethyl phthalate	1	284	194

Defects are easily caused during the tape casting process, including cracks, camber, regions of low density, surface roughness, and large pores. Table III lists the possible defects in tape casted products.

Table III. Possible Defects in Tape Casted Products[73]

In tape	In lamination	Postthermolysis
bubbles, agglomerates, surface craters, cracks, tears, warping, print break	incomplete deformation Incomplete adjoining	delamination, blister, print break

The defects come from different parts of processing. Cracks are introduced by varying shrinkages, densities, and stress gradients. The low-density regions can be caused by the retarded sintering in powder agglomerates. Surface roughness can be improved by using fine ceramic powders. Surface pores can result from the bubbles in the slurry, poor wetting ability of carriers with suspension, segregated organic materials, or pullout when samples are gathered from carriers. The incomplete deformation and adjoining process can also be caused in the lamination process.

This thesis is divided into three sections, which have been published:

1. New gelling system to fabricate complex-shaped transparent ceramics;

2. Tape-casted transparent alumina ceramic wafers;
3. Environmentally benign processing of YAG transparent wafers;

NEW GELLING SYSTEM TO FABRICATE COMPLEX-SHAPED TRANSPARENT CERAMICS

A. Introduction

The aim of this work was to prepare transparent ceramics with large size and complex-shapes by a new water-soluble gelling agent poly(isobutylene-alt-maleic anhydride). Alumina was used as an example for the application of the new gelling system. A stable suspension with 38 vol% solids loading was prepared by ball milling method. Trapped bubbles were removed before casting to obtain homogenous green bodies. The microstructure and particle distribution of alumina raw material were tested. The thermogravimetric behavior of the alumina green body was investigated, which exhibited low weight loss when compared with other gelling processes. The influence of solids loading and IB-MA addition were studied on the basis of rheological behavior of the suspension. The microstructures of alumina powders, green bodies before and after de-binding process, were compared to understand the gelling condition between alumina particles and IB-MA.

B. Experimental Procedure

A commercial alumina powder with a particle size of 0.46 μm (D50) was used as a raw material. IB-MA was used as a dispersant and gelling agent. The suspension containing 38 vol% solids was prepared by mixing alumina powders, deionized water, and IB-MA using ball milling method. After mixing, the suspension was immediately degassed in a vacuum chamber to remove trapped bubbles and then cast into molds. After consolidation and de-molding, the wet green bodies were dried at room temperature in air for 24 hours. The dried bodies were then calcined at 1273 K for 3 hours with a heating rate of 3-10 K/min. A final sintering was carried out at 2023-2123 K for 5 hours in a vacuum furnace.

The microstructure of the raw materials, green body and sintered body were observed by scanning electron microscopy (Quanta 200F, SEM, FEI Co., Hillsboro, Oregon, USA). The de-binding profile of the dried body was obtained by differential

thermal analysis (DTA) and thermogravimetric analysis (TG) in air at a heating rate of 5 K/min on the simultaneous DSC-TGA instrument (SDT 2960, DSC-TGA, TA Instruments, New Castle, Delaware, USA). The densities of green body before and after de-binding and sintering were tested by Archimedean principle.[74]

C. Results and Discussion

1. Microstructure and particle-size distribution of Al_2O_3 powders

Particle is presented by SEM in Figure 12 with the particle size observed less than 1 μm. There exist agglomerates in the Al_2O_3 powders, demonstrating the need for ball milling process.

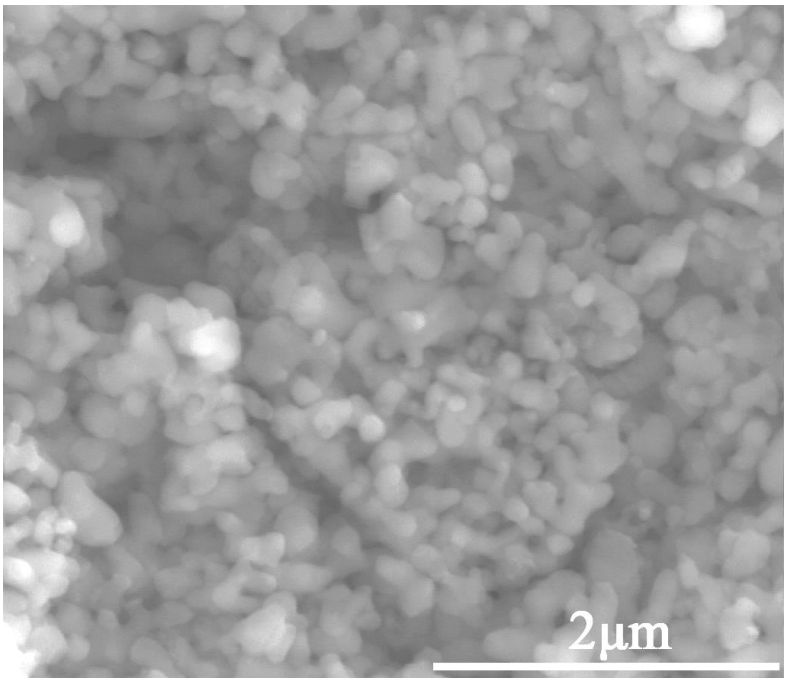

Figure 12. Microstructure of Al_2O_3 powder.

2. Viscosity change of Al_2O_3 suspension with different solids loadings and IB-MA additions

Figure 13 shows the viscosity variations of slurries containing 38 vol% Al_2O_3 as a function of IB-MA addition. A lowest viscosity was achieved with 1.24mg/m^2 addition of IB-MA. More or less addition increased the viscosities of the slurries. This phenomenon can be explained by the multifunction IB-MA. The IB-MA can function as both a gelling agent and a dispersant. The dispersion of particles in suspension relies on the steric stabilization by adsorbing of polymer on the surface of the suspending particles. The thickness of the polymer layer must be sufficient enough to prevent two particles approaching the distances where the Van der Waals attractive force dominates. Agglomeration will appear if polymer (dispersant) is not enough or too much, which can cause an increase of the viscosity.

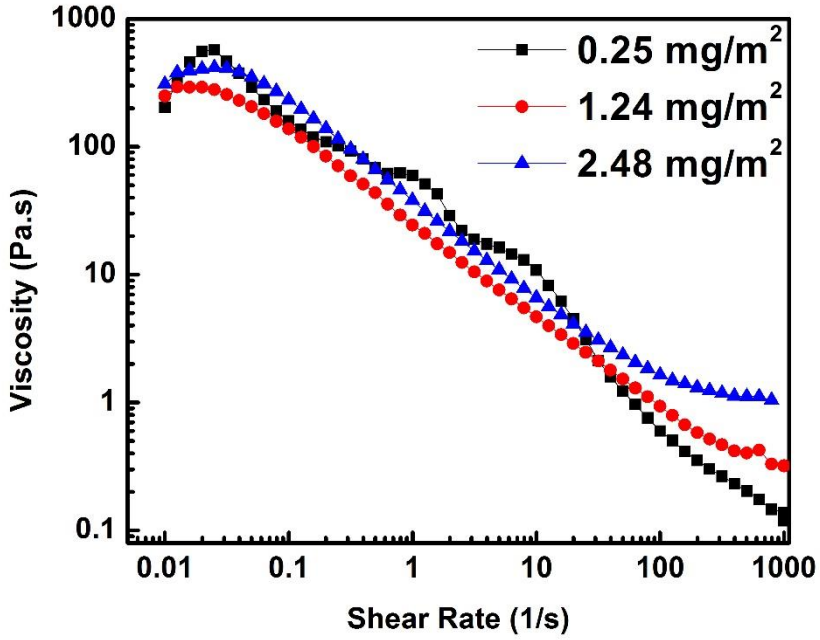

Figure 13. Viscosities of 38 vol% loading suspensions with different IB-MA additions.

Figure 14 shows the rheological curves of slurries containing IB-MA 1.24mg/m^2 with different solids loading. Higher content of solid in the slurries caused an obvious

increase of viscosity at 100 s^{-1} from 0.35 Pa•s to 1.60 Pa•s corresponding to the solids loading changing from 35 vol% to 40 vol%. All the slurries exhibit a shear-thinning behavior when the shear rate is larger than 0.03 s^{-1}, making them suitable for casting process. The thinning behavior also suggests that particle agglomerates, which tend to cause shear-thickening characteristics for the suspensions, have been destroyed at a large extent. This would promote the formation of in-situ dispersion of the particles in the suspension so that the gel-casted green bodies have more homogeneous microstructures.

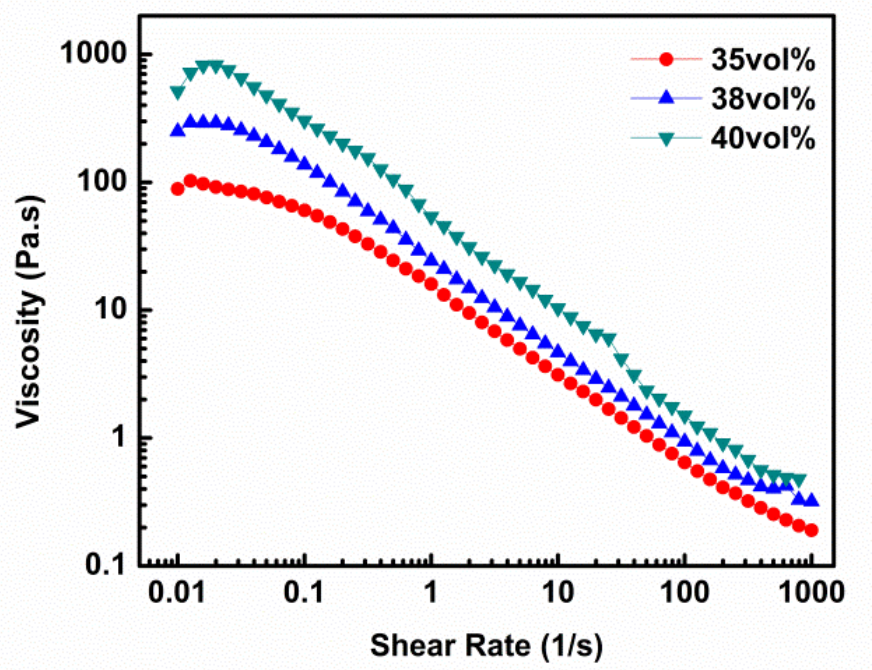

Figure 14. Viscosities of suspensions with different loadings (IB-MA 1.24mg/m^2).

3. Al_2O_3 green bodies with large size and complex shapes

By applying the spontaneous gelling agent IB-MA, samples with large size and complex shapes were made, as shown in Figure 15. The gelled samples were de-molded successfully and dried in air at room temperature without cracks. It demonstrates the spontaneous gelling agent IB-MA has potential for developing samples in larger sizes and with more complex shapes by the gelcasting technique.

Figure 15. Photos of gelled Al_2O_3 green bodies.

4. Thermogravimetric analysis

Thermogravimetric (TG) and differential thermal analysis (DTA) curves were measured in air from room temperature to 1573 K (1300 °C) with a heating rate 5 °C/min in Figure 16. The entire process exhibits low weight loss, about 1 wt%. As shown in the Figure 16, there is only one exothermal peak at 397 K (124 °C) caused by the evaporation of water in the green body, corresponding to the weight loss of 0.38% at the first stage. The endo-thermal peak around 808 K (535 °C) is shallow and wide, which demonstrates the de-binder process goes slowly even with a high heating rate (5 K/min). For this reason, we can perform the de-binder process in shorter time than other wet forming methods and thus reduce the processing time.

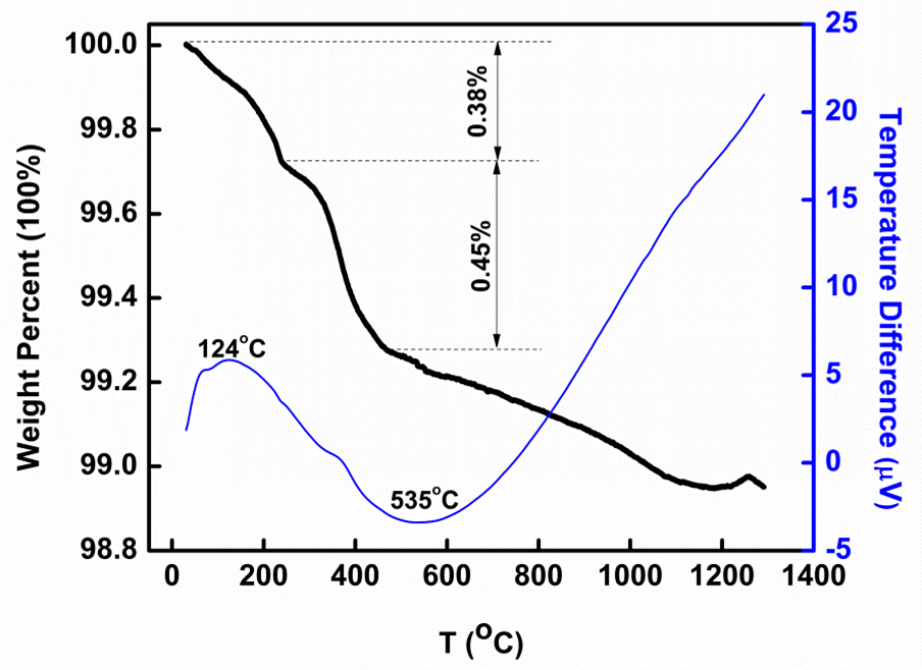

Figure 16. TG-DTA Curve of dried green body.

5. Comparison of Al_2O_3 green body gelled by using IB-MA before and after calcination.

The microstructures of Al_2O_3 green body before and after de-binding process are presented in Figure 17. Al_2O_3 powders stack closely in the gelcasted Al_2O_3 green body after drying (Figure 17(a)). After de-binding, the morphology of particles in the cross-section (Figure 17(b)) is similar to that of dried Al_2O_3 green parts.

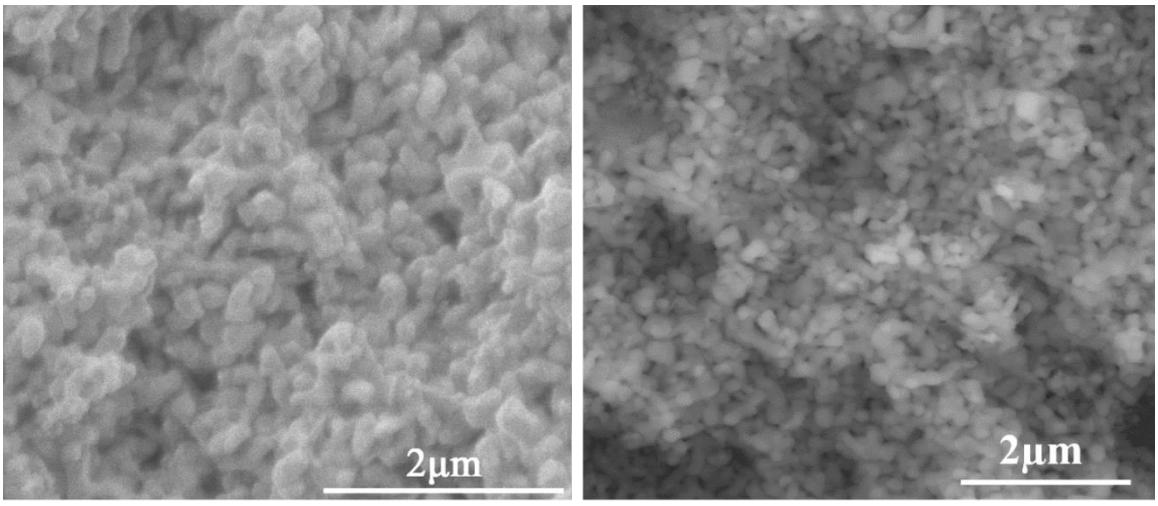

Figure 17. Comparison of the microstructure of green body before and after calcinations.

6. Density variation of Al_2O_3 during the whole process

Using the spontaneously gelcasting techniques, the relative density (ρ_{theory} = 3.981 g/cm^3) of dried ceramic parts can reach 42.65%, which is close to that after de-binding (43.05%) process. The relative density can reach 99.99% after vacuum sintering at 2023-2123 K for 5 hours.

7. Translucent Al_2O_3 after vacuum-sintering

As shown in Figure 18, after vacuum-sintering at 2023-2123 K for 5 hours, translucent Al_2O_3 was achieved. The microstructure (Figure 19) shows that a dense Al_2O_3 ceramic without pores was sintered with grain size distributed between 30-80 μm. It can verify that the spontaneous gelling agent IB-MA can be used to make full-density ceramics, translucent, and transparent ceramics.

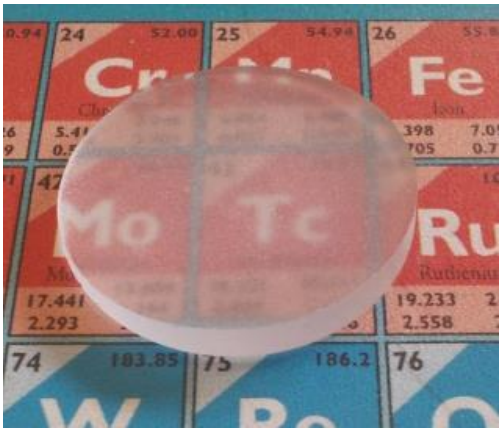

Figure 18. Photo of vacuum-sintered Al_2O_3 ceramic (without polishing).

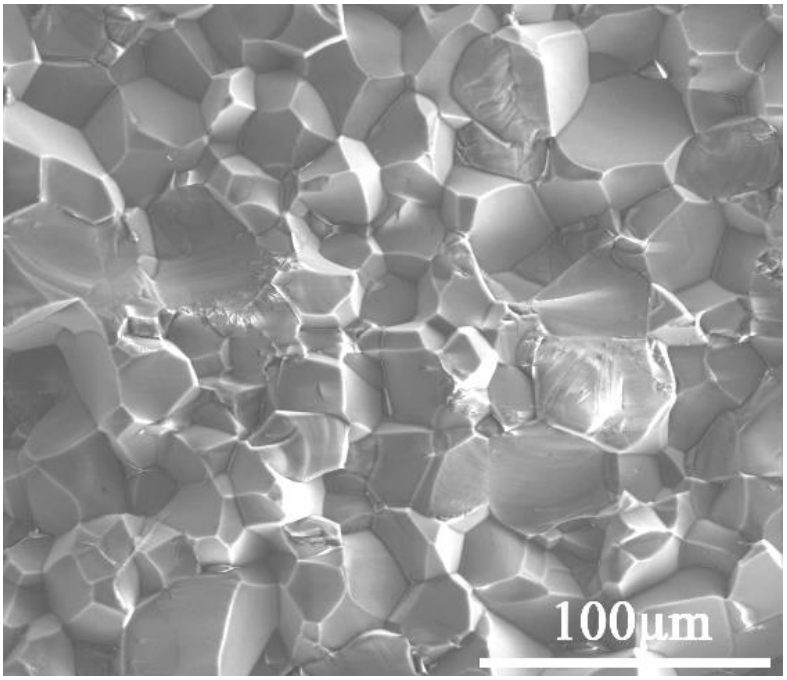

Figure 19. Microstructure image of the fresh fracture surface of vacuum-sintered Al_2O_3

D. Conclusion

IB-MA gelcasting process can be used to produce ceramic parts with large or complex parts after the final sintering. The entire process is simple and green to the environment. The de-binding process and sintering can be finished a heating rate as high

as 3~10 K/min. Translucent Al_2O_3 with a relative density of 99.99% can be made using new spontaneous gelling agent IB-MA and the final vacuum sintering techniques at after vacuum-sintering at 2023-2123 K for 5 hours. The relative density of the vacuum-sintered ceramics can reach 99.99%.

TAPE-CASTED TRANSPARENT ALUMINA CERAMIC WAFERS

A. Introduction

Ceramic wafers of alumina (Al_2O_3) were produced by tape casting of aqueous slurry followed by vacuum sintering. The binder system used is an isobutylene copolymer and maleic anhydride, which is an environmentally friendly organic. The rheological properties of the slurries were studied as a function of slurry solid loading and binder addition level. Through the optimization of plasticizer addition, green tapes were casted with excellent plasticity and a thickness of 240-740 μm. The tapes displayed a post-sintering thickness of 150-660 μm. The powder morphologies, and the fracture surface and as-sintered surface of Al_2O_3 wafers, were examined by scanning electron microscopy (SEM). The in-line transmittance of the transparent unpolished Al_2O_3 wafers with a thickness of 660 μm was found to be 72% at a wavelength of 5 μm and 26% at the wavelength of 600 nm.

B. Experimental

Commercial Al_2O_3 powders (CR-10, Baikowski International Corp., Annecy, France) were used as raw materials. A water solvable copolymer IB-MA with density 1.3 g/cm^3 (M.W. = 160000~300000, Kuraray Co., LTD., Osaka, Japan), was used as both a binder and a dispersant. Tape casting slurries were prepared with Al_2O_3 powder, IB-MA and distilled water by ball-milling to achieve homogeneous dispersion of the different components. Slurries with different binder levels and solids loading were prepared. The viscosities of the slurries were investigated to understand the effect of the variables on rheological behaviors, using a stress-controlled rheometer (AR2000, Rheometer, TA Instruments, New Castle, Delaware, USA). Viscosity measurements were performed by pre-shearing the slurry at 100 s^{-1} for 30 s and increasing the shear rate continuously from 0.001-200 s^{-1}. The experimental process for producing wafers is shown in Figure 20, as is much simpler than many other tape casting systems [54,75-78]. After de-gassing, the Al_2O_3 slurries were tape-casted with a moving blade at speed of 2 cm/s on a stationary polypropylene carrier film (Mylar) with blade gaps 0.5mm to 1.5mm. After de-molding

and drying, the de-binding and pre-sintering of the green sheets was carried out with heating rates of 3-5 K/min to 1273 K for 3-5 hours. The final alumina ceramics was sintered in vacuum furnace (10^{-5}-10^{-6} MPa) at 2023-2123 K for 3-5 hours with heating rate of 10 K/min.

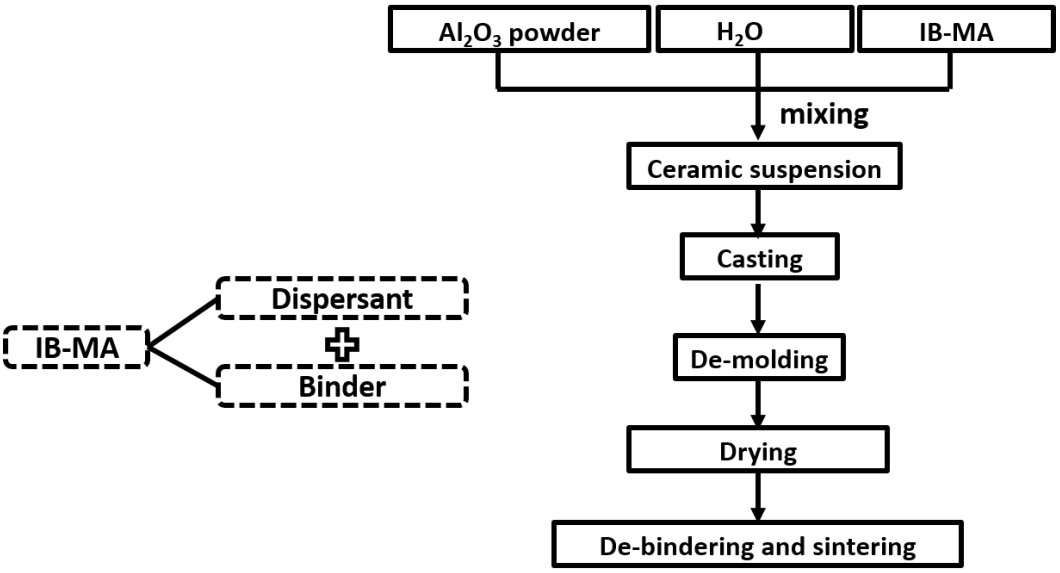

Figure 20. Flowchart for transparent Al_2O_3 by tape casting and vacuum sintering techniques.

The morphology of Al_2O_3 powders, as well as the fracture surface and as-sintered surface were observed using scanning electron microscopy (Quanta 200F, SEM, FEI Co., Hillsboro, Oregon, USA). The microstructures of the fracture and surface of vacuum sintered Al_2O_3 ceramics were examined by scanning electron microscopy (Quanta 200F, SEM, FEI Co., Hillsboro, Oregon, USA) together with the in-line transmittance in the ultraviolet-visible light region using UV-VIS spectrometer (Perkin Elmer Lambda 950, PerkinElmer, Inc., Waltham, Massachusetts, USA) and the infrared region tested using Fourier transform infrared (FTIR) spectrometer (Nicolet 6700, Thermo Fisher Scientific Corp., Waltham, Massachusetts, USA).

C. Results and discussion

1. Powder characterization

Figure 21 exhibits morphology of commercial Al_2O_3 powders with the particle size less than 1 μm. Agglomerations in the powder are apparent, which further reinforces the necessity of ball milling to achieve slurry homogeneity.

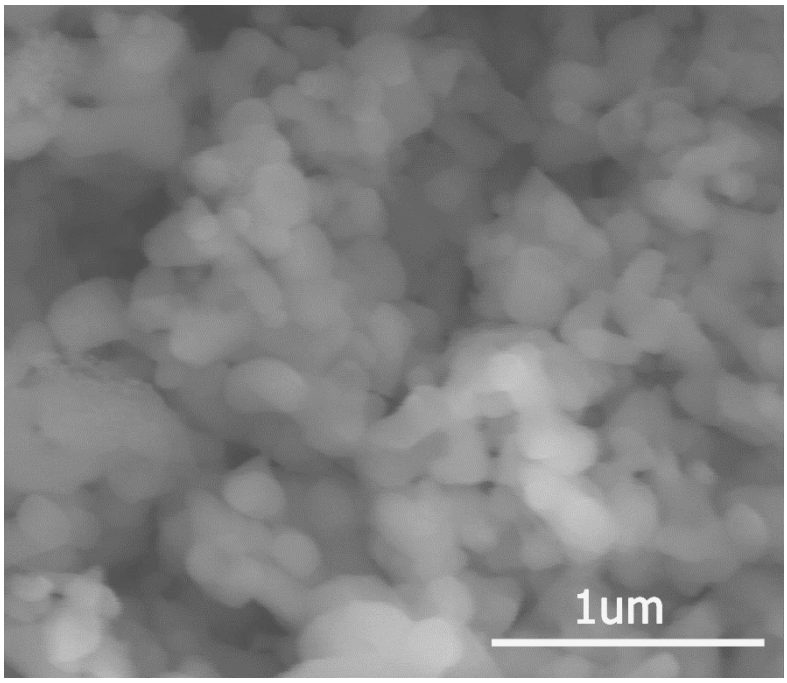

Figure 21. Particle morphology images of Al_2O_3 powder CR-10.

2. Rheological properties of Al_2O_3 slurries

The rheological behavior of the slurries is influenced by ceramic powders, as well as dispersant, binder, solvent and other organic additives that are used. However, the most important factor is binder addition level.[50,53] The influence of the high surface tension of water, as well as limited solubility of binders also need be considered in aqueous system. To decrease the deformation and defects during the drying and firing process, the water and binder content should be as low as possible, as water and organic

additives need to be removed before final sintering. Here, IB-MA works as both a binder and a dispersant for Al_2O_3 ceramic powder. The rheological behaviors of the slurries were examined as a function of IB-MA level and solids loading.

(1) Viscosities of Al_2O_3 slurries with respect to the IB-MA addition

The rheological properties of Al_2O_3 slurries (weight ratio of water : Al_2O_3 powder = 3:8) were examined by analyzing the change in viscosities over IB-MA addition level of 15-25 wt% (water based) at 298 K in air, as shown in Figure 22.

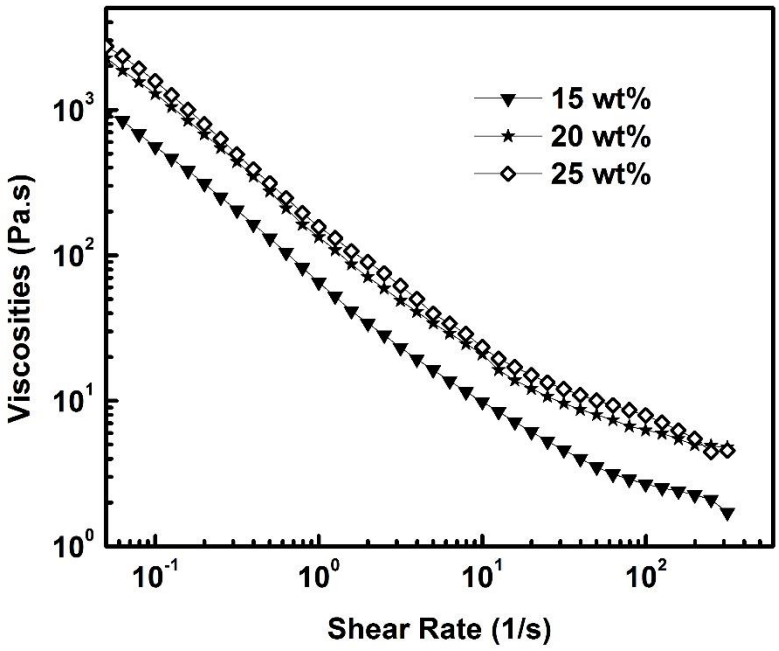

Figure 22. Viscosities of Al_2O_3 slurries varying with binder addition (water based) with solid loading 35 vol%.

The viscosity curve in Figure 22 shows that these Al_2O_3 slurries exhibit shear thinning behavior (pseudoplasticity) at shear rates 0.05-200 s^{-1}, which is similar to other reports. [33,35,71] During the tape casting process, the doctor blade moves at a speed of 2 cm/s to ensure minimal influences of shear rate changes on the viscosity, which is decided by the gradient of viscosity versus shear rate[79] in Figure 22. The maximum shear

rate of 2 cm/s is 20 s^{-1} for the doctor blade height 1mm and 40 s^{-1} for 0.5 mm, calculated by:[80]

$$\dot{\gamma}_{max} = \frac{v}{h} \quad (1)$$

Where *h* is the doctor blade height and *v* is the doctor blade velocity.

Pseudoplasticity behavior is crucial for the tape casing process for following reasons: (1) High shear rates produce low viscosities to ensure the homogeneous mass flow in the slurries; (2) Moving doctor blade can produce enough shear force to decrease the viscosity followed by a rapid increase after the blade stops to suppress uncontrolled flow and sedimentation of ceramic powders.

In Figure 22, the viscosities of slurries increase with binder addition level in the range from 15 wt% to 20 wt%, while remaining relatively constant over the range of 20-25 wt%. It can be found that when binder addition was less than 20 wt%, the binder addition level has a large influence on the rheological behavior while a minor influence when it was 20 wt% or greater. Therefore, 20 wt% can be chose as the IB-MA concentration for aqueous tape casting process.

(2) Viscosity of Al_2O_3 slurries varying with solids loadings

The viscosities of Al_2O_3 slurries with IB-MA concentration 20 wt% (powder weight based) were examined as a function of solids loading, as shown in Figure 23. From the viscosity curves (Figure 23), it can be seen that all the Al_2O_3 slurries show shear thinning process (pseudoplasticity), similar to the rheological behaviors of the suspensions shown in the inset of Figure 22. The viscosities show a large increase over the range of 30 vol% to 39 vol%. High solids loading is desirable in tape casting process, as it helps to keep the shape of cast tape and reduces drying shrinkage, deformation and cracks. The slurry viscosity with solids loading 30 vol% is as low as 25 Pa•s during the shearing process, which may introduce flow receding in the tapes. This may also cause droplet formation, the larger shrinkage and more complex drying process. However, high solids loading can trap bubbles in the degassing process. The viscosity of Al_2O_3 slurry

with solid loading of 39 vol% was as high as 32000 Pa•s, which made it difficult to mix by ball-milling and the following casting process. However, the slurries with solid loading of 35 vol% showed moderate viscosity, which is suitable for this tape casting process. Based on the discussion above, the Al_2O_3 slurry with 20wt% binder addition level and 35 vol% solid loading was adopted for tape casting process under doctor blade speed of 2 cm/s.

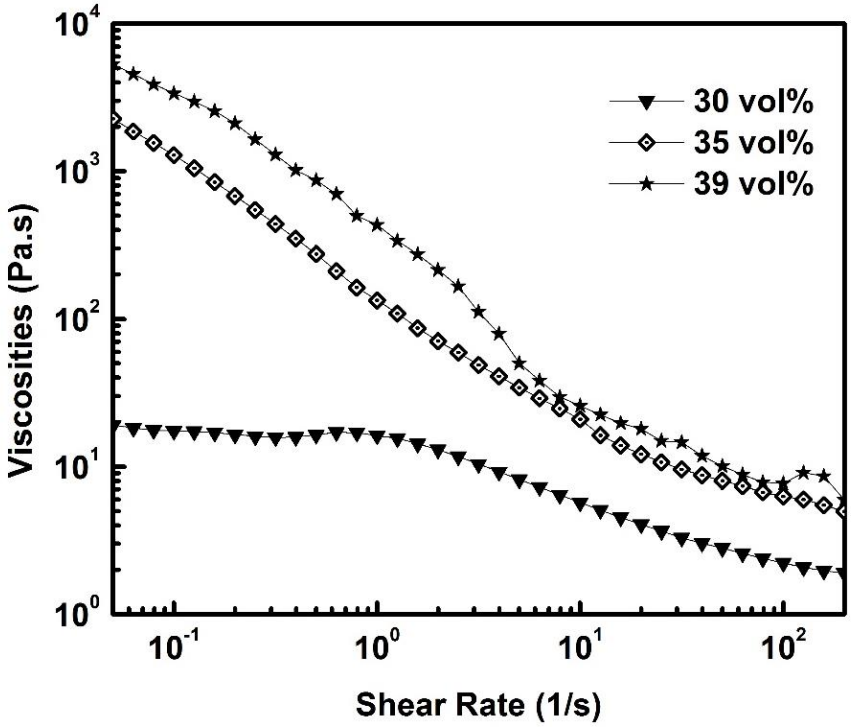

Figure 23. Viscosity of Al_2O_3 slurries varying with different solids loadings with binder addition 20wt%.

3. Characterization of Al_2O_3 green tapes

To improve the plasticity and workability of the green tapes, plasticizers were added to improve the flexibility of the tapes by lower the glass transition temperature (T_g). Photographs of good quality green tapes casted with a solid loading of 35 vol% and

binder addition level of 20 wt% are shown in Figure 24. The Al_2O_3 green tapes were flexible, easy to handle, and without any cracks after twisting.

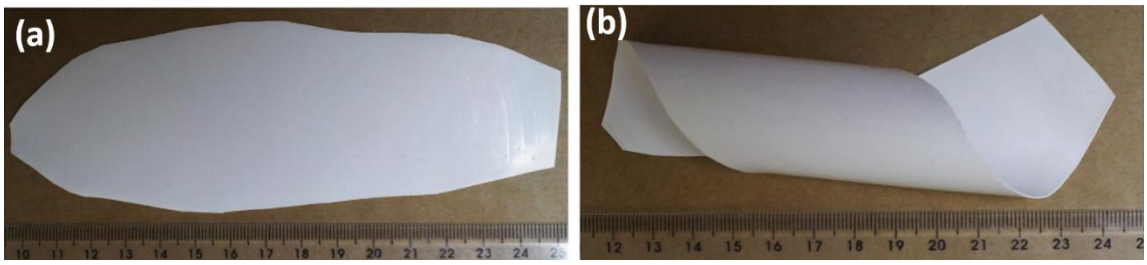

Figure 24. Photos of Al_2O_3 green tape after casting in air at room temperature (a) Flat green tape; (b) Flexible green tape.

The microstructures of Al_2O_3 tape surfaces, derived from the slurries containing 35 vol% solid loading with 20 wt% binder addition, before and after de-binding process are shown in Figure 25. It can be observed that uniform green body was achieved by the IB-MA tape casting process. Al_2O_3 particles are homogeneously distributed and encapsulated by binders after tape casting, without any agglomerates, giving rise to improved density and strength of the green tape. The binder burnout process was performed at heating rate of 2-5 K/min without defects (e.g. deformation, blister or cracks, etc.), which are commonly observed with excessive heating rates in other tape casting processes, [77,81] which shortens the de-binding process and save production time and energy. During de-binding process, packing density was increased through the removal of all organic material.

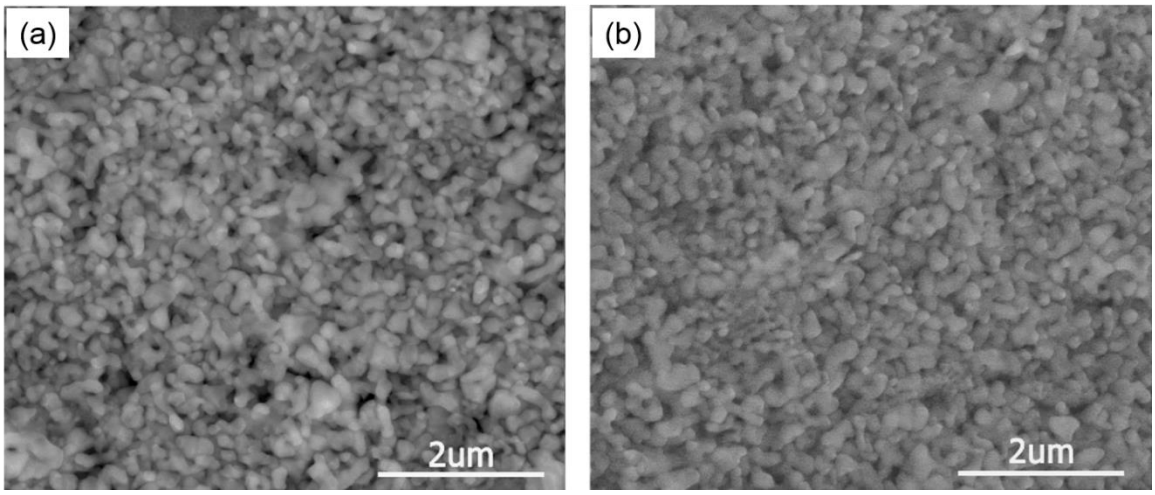

Figure 25. Microstructure of Al_2O_3 green tape (a) before and (b) after debinding process.

4. Vacuum sintering of transparent Al_2O_3 tape

Transparent Al_2O_3 wafers were achieved by final vacuum sintering at 2023-2123 K for 3-5 hours Figure 26. The obtained transparent Al_2O_3 wafers show good quality and defect-free surfaces. Figure 27 shows the surface and fracture microstructures of transparent Al_2O_3 wafers. The main grain size distribution lies in the range of 20-80 μm, which was statistically calculated using software (Nano Measurer, Version 1.2, Department of Chemistry, Fudan University, Shanghai, China). No obvious differences are observed in the microstructure of Al_2O_3 wafers between casting direction, transverse-to-casting direction and thickness direction. The grains compact together very tightly without any pores on the grains or grain boundaries in the surface or fracture plane. In Figure 27(b), transparent Al_2O_3 wafers are dominated by inter-granular fracture with minor intra-crystalline rupture. The sintered thickness of a wafer is shown to be about 660 μm in the inset of Figure 27(b).

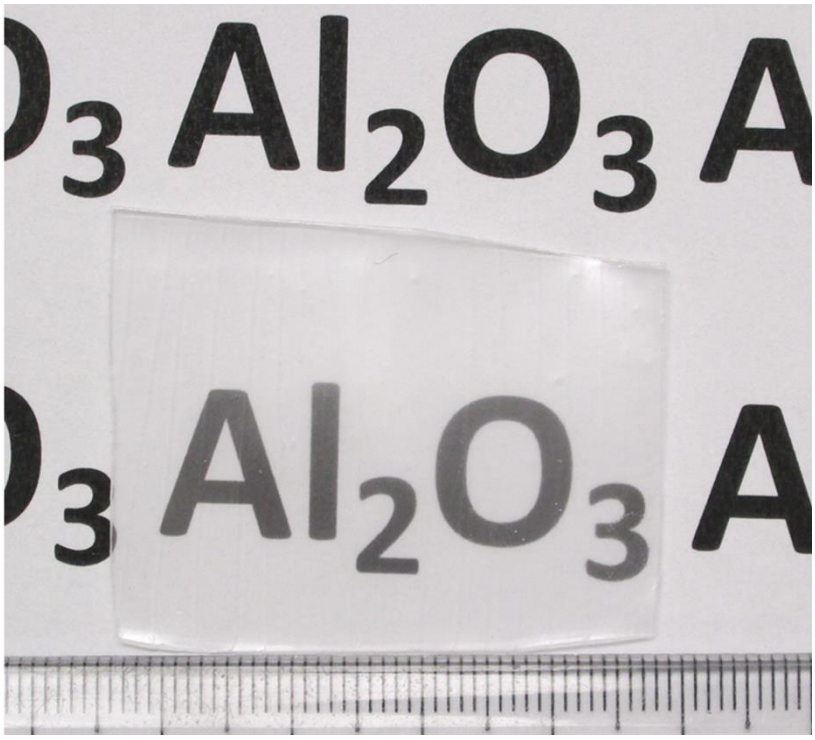

Figure 26. Photo of transparent Al_2O_3 ceramics (vacuum sintered (10^{-5}-10^{-6} MPa) at 2023-2123 K for 3-5 hours with heating rate of 10 K/min).

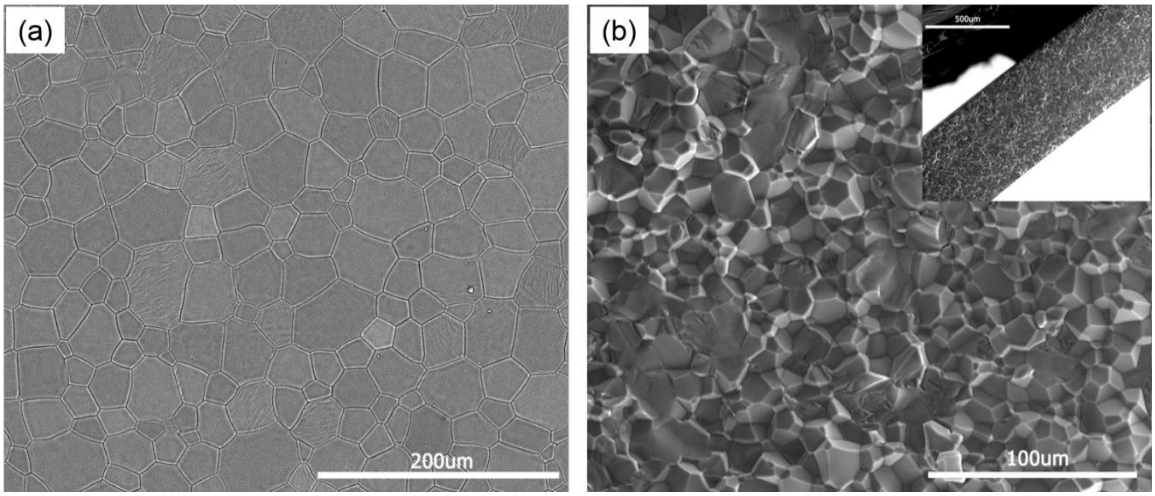

Figure 27. Microstructures of transparent Al_2O_3 ceramics (a)surface; (b)fracture surface.

5. Transmittance test of tape-casted and vacuum sintered transparent Al_2O_3 wafers

The in-line transmittance of tape-casted and vacuum sintered transparent Al_2O_3 wafers without polishing was characterized in UV-VIS region (200-800 nm) in Figure 28 and IR region (3-10 μm) in Figure 29. In UV-VIS region, the in-line transmittance increases gradually from 33% to 43% (Figure 28) with increasing incident wavelength. The transmittance of transparent Al_2O_3 (without polishing) at 600 nm is about 39%, better than results of epoxy resin gelcast translucent Al_2O_3[9,35]. In IR region (3-10 μm), the in-line transmittance has a value of 82% at 5 μm (Figure 29), which increases between 3-5 μm and decreases over the range of 5-8 μm. An obvious absorption peak at 4.2 μm might come from the C-O bonding stretching[82].

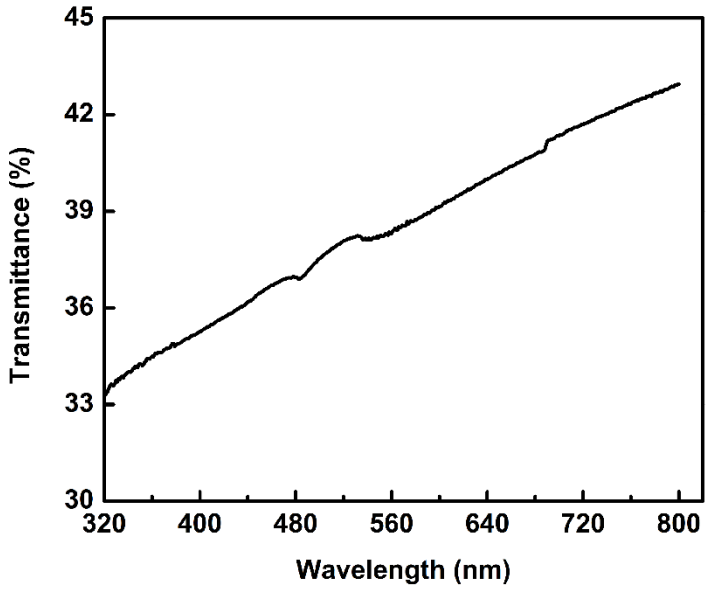

Figure 28. In-line transmittance of transparent Al_2O_3 (vacuum sintered (10^{-5}-10^{-6}MPa) at 2023-2123 K for 3-5 hours with heating rate of 10 K/min; Thickness: 660μm, no polishing) in UV-VIS region.

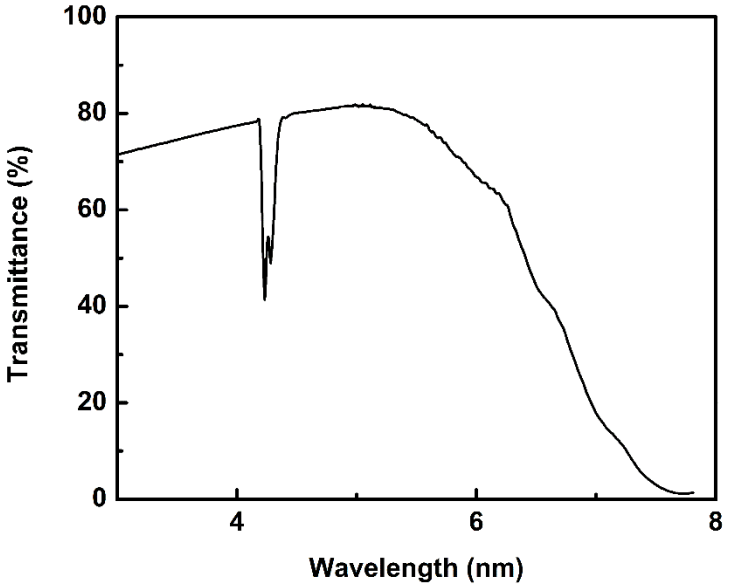

Figure 29. In-line transmittance of transparent Al_2O_3 (vacuum sintered (10^{-5}-10^{-6}MPa) at 2023-2123 K for 3-5 hours with heating rate of 10K/min; Thickness: 660μm, no polishing) in IR region.

D. Conclusion:

Transparent Al_2O_3 wafers were fabricated by tape casting with a new environmentally friendly binder (IB-MA) followed by vacuum sintering techniques. The binder IB-MA can function as both dispersant and binder for the tape casting process. A binder addition level of 20 wt% and solid loading of 35 vol% Al_2O_3 were found to be optimum conditions for aqueous tape casting and production of flexible green tapes. Green tape with good plasticity was made successfully. After de-binding and vacuum sintering process, transparent Al_2O_3 wafers with transmittance of 39% at 600 nm and 82% at 5 μm were successfully produced. Average grain size of final wafers is about 10-80 μm without apparent pores microstructures. The results indicate that environmentally friendly IB-MA can be potentially applied for tape casting of transparent ceramics.

ENVIRONMENTALLY BENIGN PROCESSING OF YTTRIUM ALUMINIUM GARNET (YAG) TRANSPARENT WAFERS

A. Introduction

Transparent yttrium aluminum garnet (YAG) wafers were successfully produced via aqueous tape casting and vacuum sintering techniques using a new environmentally friendly binder, a copolymer of isobutylene and maleic anhydride (IB-MA). Aqueous YAG slurries were mixed by ball-milling, which was followed by de-gassing and tape casting of wafers. The final YAG green tapes were homogenous and flexible, and can be bent freely without cracking. After the drying and sintering processes, transparent YAG wafers were achieved. The microstructures of both the green tape and vacuum-sintered YAG ceramic were observed by scanning electronic microscopy (SEM). Phase composition were examined by X-ray diffraction (XRD). Optical transmittance was measured in UV-VIS regions with the result that the transmittance is 82.6% at a wavelength of 800nm.

B. Experimental

1. YAG slurries preparation

High-purity powders of α-Al_2O_3 (CR-10, Baikowski International Corp., Annecy, France), Y_2O_3 (99.99%, Sigma-Aldrich Corp., St. Louis, Missouri, USA), and IB-MA (ISOBAM, Kuraray Co., LTD., Osaka, Japan) were used as raw materials. YAG slurries with solid loading of 28 vol% were mixed by ball-milling with zirconia grinding media at a speed of 200-300 rpm for 3 hours. After the addition of plasticizer, the slurry was cast on a stationary Mylar carrier with a moving doctor blade at a speed of 0.8-2.8 cm/s. After drying in air for 24 hours at room temperature, the green tapes were without deformation or cracking. After de-molding and drying, the ceramic green tapes were de-binded at 1073-1273 K for 3 hours, at a ramp rate of 2-5 K/min. Final sintering was performed in a vacuum atmosphere (10^{-5}-10^{-6} MPa) at a temperature of 1973-2073 K for 3 hours, at a ramp rate of 2~10 K /min.

2. Characterization for the slurries and ceramic wafers

The rheological properties of the produced slurries were measured with a rotational stress-controlled rheometer (AR2000, Rheometer, TA Instruments, New Castle, Delaware, USA) in continuous shear rate mode in the region of 0.01-1000 s^{-1}, at 298 K. The YAG green tapes were very flexible and can be bent and twisted freely. The surface and cross-sectional microstructure of the YAG green tapes and vacuum-sintered wafers were examined via scanning electron microscopy (Quanta 200F, SEM, FEI Co., Hillsboro, Oregon, USA). Phase compositions of YAG green body and vacuum-sintered wafer were tested by X-ray diffraction (XRD) (Bruker D2 Phaser, Madison, Wisconsin, USA) equipped with a Cu radiation (λ= 0.154 nm) in the range of 2θ=10~75 °. The in-line transmittance of the wafers was measured in the UV-VIS region using UV-VIS spectrometry (Perkin Elmer Lambda 950, PerkinElmer, Inc., Waltham, Massachusetts, USA).

C. Results and discussion

1. Rheological property

The rheological behavior of the tape casting YAG slurries with solid loading of 28 vol% was measured over shear rate range of 0.1-1000 s^{-1}, the results of which are shown in Figure 30. The measured YAG slurries displayed shear thinning behavior over the entire measured region, which is desirable for tape casting process.

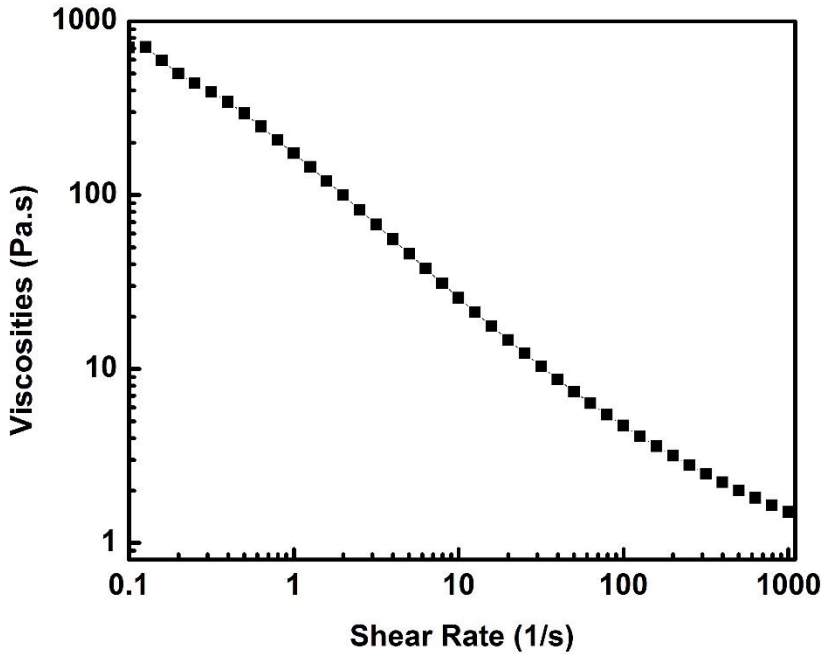

Figure 30. Viscosity of YAG slurry with solid loading 28 vol% varying with shear rate.

High viscosities were achieved at low shear rates, which can prevent particle flocculation and sedimentation. At high shear rate, the measured viscosities were relatively low, which is desirable in the actual forming step of tape casting. For example, the viscosity is less than 10 Pa·s at a shear rate higher than $20s^{-1}$. The low viscosity of the ceramic slurry at high shear rates can ensure the homogeneous dispersion of the slurry system, and high viscosity at static state to keep the dimensional accuracy.

The shear thinning behavior of ceramic based suspensions used in tape casting can also be described by the equation below:[83]

$$\tau = k\,(r)^n \qquad (2)$$

Where τ is the shear stress, r is the shear rate and n is a value, which is unique to the material system and less than one. The value of n can be calculated from the slope of log-log curve in Figure 30, which is less than one and consistent with Equation (2).

2. Tape casting of the YAG green wafer

In the tape casting step, the casting was performed at a speed of 0.8-2.8 cm/s, similar to speeds reported in the literature for other water-based systems. [41,77] Without the addition of surfactant, all slurries wet the Mylar carrier well and were "locked" onto the carrier to prevent the slip from receding and forming droplets. After drying for 2 hours on the Mylar carrier, the green tapes (Figure 31a) were easy to remove from the carrier film. No cracks, blisters or pinholes were observed in the green tape, and all had smooth surfaces. In addition, the tapes were smooth, flexible, and easy to handle (Figure 31b).

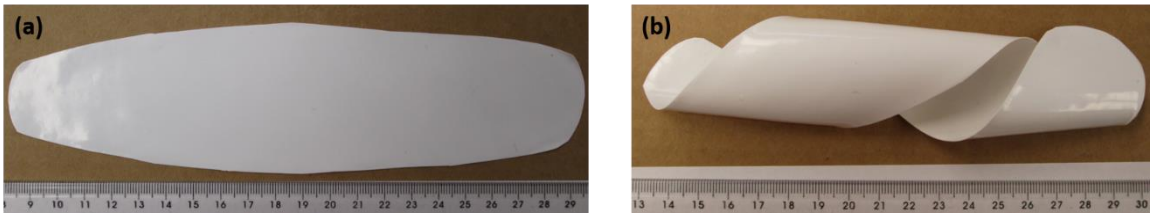

Figure 31. Photographs of the YAG green tape after de-molding at room temperature.

3. Microstructure research of green body and vacuum sintered YAG wafer

Shown in Figure 32 are the fracture surfaces of YAG tape after de-binding (Figure 32a) and vacuum sintering (Figure 32b). The particles in the fracture surfaces of the de-binded YAG green tapes are distributed homogeneously without any agglomerates. As shown in Figure 32b, the sintered YAG wafers show fully densified microstructure. The grains densified uniformly with grain size distribution of 1.5-5 μm, which was statistically calculated using software (Nano Measurer, Version 1.2, Department of Chemistry, Fudan University, Shanghai, China). No differences in microstructure were observable between the casting and transverse direction. The fracture

mode of the vacuum sintered YAG wafers appeared to be mainly trans-granular for large grains, as well as minor inter-granular for small grains within the grain size range of 1-3 μm. There were no obvious bubbles in the fracture surface of the sintered YAG ceramic. According to measurement, the relative densities of the green body and vacuum sintered body were measured with the results ~54.5% for the green body and 99.5% for the vacuum-sintered sample.

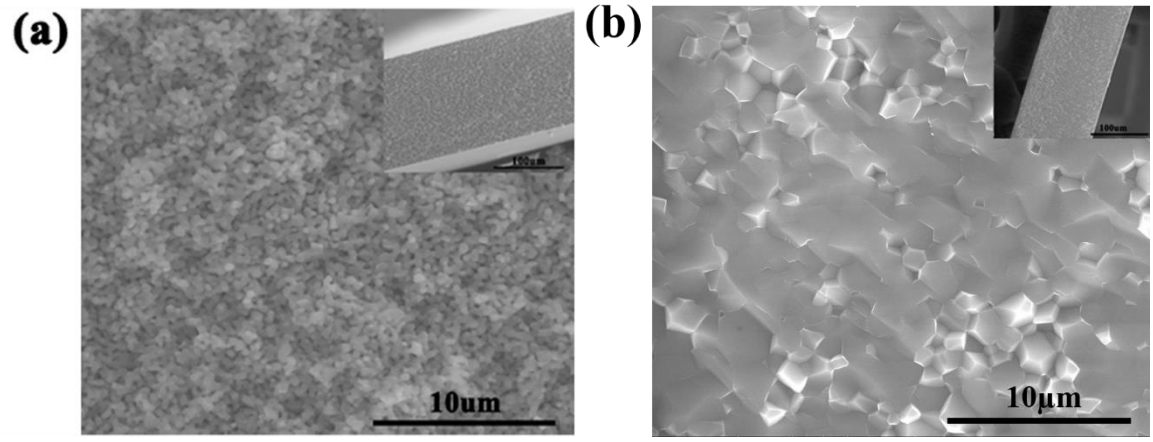

Figure 32. Microstructure of fracture surfaces of YAG tape after (a) de-binding at 1073-1273 K for 3 hours and (b) vacuum sintering at 1973-2073 K for 3 hours.

4. Phase identification

Figure 33 shows the phase composition of the tape-casted green tape after de-binding in air at 1073-1273 K for 3 hours and the vacuum-sintered YAG at 1973-2073 K for 3 hours. For the Al_2O_3-Y_2O_3 system, three phases, including YAM ($Y_4Al_2O_9$), YAP ($YAlO_3$), YAG ($Y_3Al_5O_{12}$), can be obtained during the different temperature region, reported by Kinsman *et al.*[84]

$$2Y_2O_3+Al_2O_3 \rightarrow Y_4Al_2O_9 \qquad 1173 - 1373\ K \tag{3}$$

$$Y_4Al_2O_9+Al_2O_3 \rightarrow 4YAlO_3 \qquad 1373 - 1523\ K \tag{4}$$

$$3YAlO_3+Al_2O_3 \rightarrow Y_3Al_5O_{12} \qquad 1673 - 1873\ K \tag{5}$$

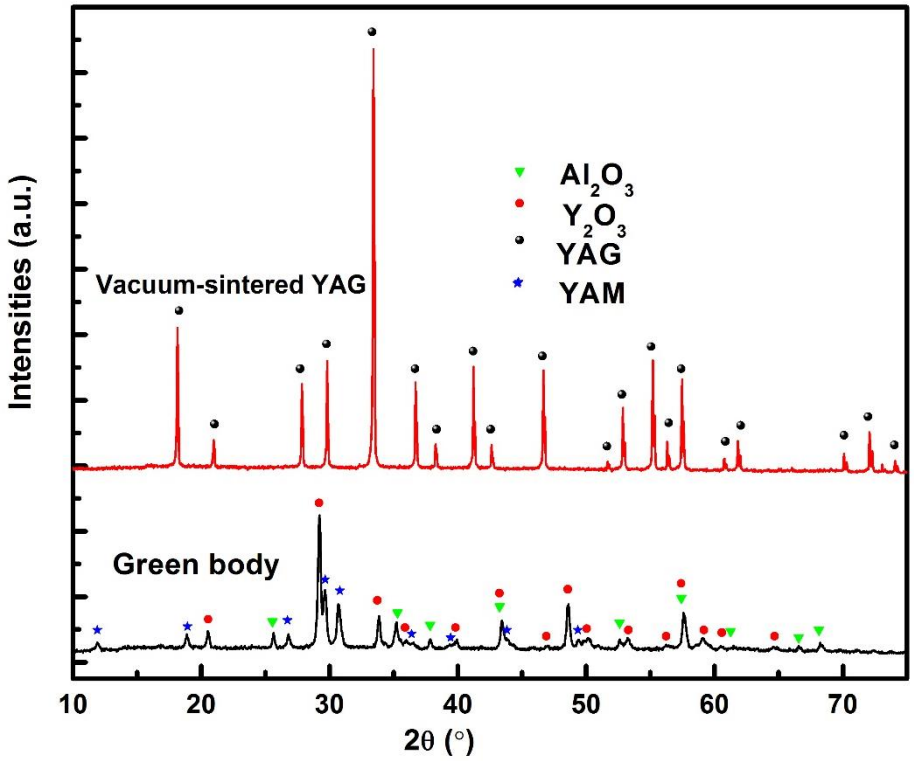

Figure 33. X-ray diffraction pattern of YAG green body (1073-1273 K, 3 hours) and vacuum-sintered wafer (1973-2073 K, 3 hours).

In Figure 33, after de-binding at 1073-1273 K for 3 hours, YAM was observed co-existed with unreacted Y_2O_3 and Al_2O_3. After the vacuum sintering at 1973-2073 K, YAG is the only phase detected, indicating the totally reaction of Y_2O_3 and Al_2O_3.

5. Optical transmittance of vacuum-sintered YAG wafer

A photo of a vacuum sintered sample with a thickness of 0.26 mm is shown in the inset of Figure 34. The YAG chips also display excellent optical properties, and the in-line transmittance was measured to be about 82.6% at a wavelength of 800 nm. These results verify that the IB-MA tape casting system can be successfully used for the production of thin tapes with excellent preservation of optical properties.

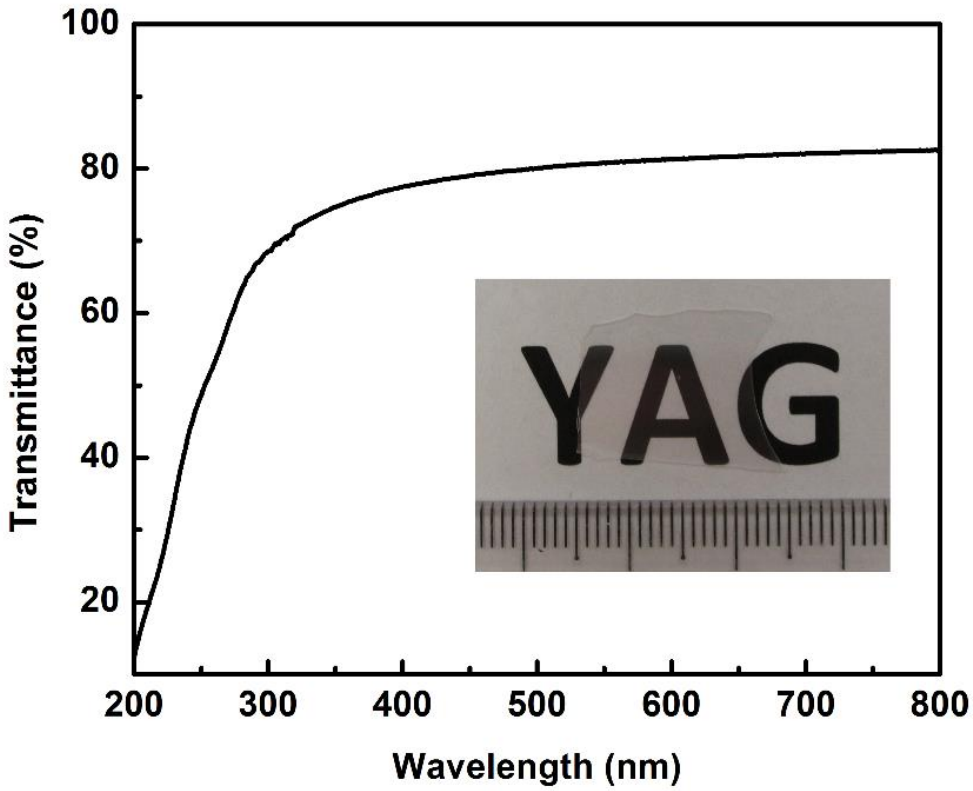

Figure 34. Transmittance of vacuum-sintered (1973-2073 K, 3 hours) YAG chips formed by aqueous tape casting methods using IB-MA as binder.

D. Conclusion

Transparent YAG wafers were successfully processed by tape casting with IB-MA as binder and the vacuum-sintering techniques. Slurries produced with IB-MA tape casting system show shear thinning behavior in the region of 0.1-1000 s^{-1}. The final green tape is flat, smooth, flexible, and easy to handle. The microstructure of the green tape is homogeneous without any observable agglomeration. The vacuum sintered YAG ceramic is uniform in both the casting and lateral direction with a grain size distribution of 1.5-5 μm and transmittance of 82.6% at the wavelength of 800 nm.

SUMMARY AND CONCLUSIONS

A new binder, IB-MA, was estimated for aqueous ceramic processing. IB-MA is a multifunctional, water-soluble, and environment-friendly copolymer of isobutylene and maleic anhydride.

IB-MA can work as a good dispersant and a spontaneous gelling agent for ceramic powder to produce homogeneous ceramic slurries. With IB-MA as the dispersant for Al_2O_3 powder (d_{50} = 0.46 μm) Al_2O_3 ceramic slurries with solid loading as high as 40 vol% were successfully made. Ceramic green bodies with large size and complex shapes were obtained using IB-MA gelling techniques. After vacuum sintering, translucent Al_2O_3 with a relative density of 99.985% was achieved. The grains pack densely in the vacuum sintering process without any pore observed on the cross-section part.

IB-MA can also work as a binder for aqueous tape casting process. IB-MA can produce enough strength to the ceramic green body, provide formability, and keep the ceramic powders in the desired shapes.

Adopting IB-MA aqueous tape casting process, transparent Al_2O_3 wafers were fabricated after de-binding and final vacuum sintering process. The binder ISOBAM can function as both a good dispersant and a binder for the Al_2O_3 tape casting process. Al_2O_3 ceramic suspension with the IB-MA addition level of 20 wt% and solid loading of 35 vol% Al_2O_3 were found to be the optimum conditions for this aqueous tape casting process. High quality ceramic green tape with good flexibility were produced successfully. Transparent Al_2O_3 wafers with the in-line transmittance of 39% at 600 nm and 82% at 5 μm were successfully made after the final vacuum sintering process. The average grain size of final wafers is about 10-80 μm without apparent pores on the microstructure of wafer surface.

Transparent YAG wafers were also successfully processed by IB-MA tape casting system with IB-MA as the binder and the final vacuum-sintering process. The obtained YAG green tape is very flat, smooth, flexible, and easy to handle. The microstructure of the green tape is homogeneous without any observable agglomeration. The vacuum sintered YAG ceramic wafer is uniform in both the casting and lateral direction with a

grain size distribution of 1.5-5μm and transmittance of 82.6% at the wavelength of 800 nm.

PUBLICATION LIST

- Yan Yang, Yiquan Wu, "Tape-casted transparent alumina ceramics wafers", Journal of Material Research, 29(19), **2014**, 2312-2317

- Yan Yang, Yiquan Wu, "Environmentally benign processing of YAG transparent wafers", Optical Materials, accepted.

- Yan Yang, Yiquan Wu, "New gelling system to fabricate complex-shaped transparent ceramics", *SPIE Proceedings* 8708, Window and Dome Technologies and Materials XIII, 8708D, **2013**

- Shi Chen, Yiquan Wu, Yan Yang, "Spark plasma sintering of hexagonal structure Yb^{3+}-doped $Sr_5(PO_4)_3F$ transparent ceramics", *Journal of the America Ceramic Society*, 96(6), **2013**, 1694-1697

- Yan Yang, Hua Wei, Lihua Zhang, Kim Kisslinger, Charles L. Melcher, Yiquan Wu, "Blue emission of Eu^{2+}-doped translucent Alumina", *Journal of Luminescence, submitted*

- "Reduction of Eu^{3+} to Eu^{2+} in vacuum-sintered translucent Al_2O_3", *to be submitted*

- "Strong red-emission of flower-like Eu^{3+}:$Li_4TI_5O_{12}$ powders for potential phosphor applications", to be submitted

REFERENCES

1. U. Kim and W. M. Carty, "The Effect of Polymer Compatibility on the Binder Migration During Spray Drying"; pp. 33-41, Vol. 23, *Materials & Equipment/Whitewares: Ceramic Engineering and Science Proceedings.* Edited by W. M. Carty. John Wiley & Sons, Inc., Westerville, OH, 2002.

2. N. Ninos and W. M. Carty, "Using Surface Area to Solve an Inappropriate Mixing Problem"; pp. 79-85, Vol. 25, *Materials & Equipment/Whitewares: Ceramic Engineering and Science Proceedings.* Edited by W. M. Carty. John Wiley & Sons, Westerville, OH, 2001.

3. C. R. August and R. A. Haber, "Benbow Analysis of Extruded Alumina Pastes"; pp. 15-21, Vol. 25, *Whitewares and Materials: Ceramic Engineering and Science Proceedings.* Edited by W. M. Carty. John Wiley & Sons, Inc., Westerville, OH, 2004.

4. B. C. Mutsuddy, Ford, Renee G., *Ceramic Injection Molding,* Chapman & Hall, London, UK, 1995.

5. E. Sachs, M. Cima, J. Bredt, A. Curodeau, T. L. Fan, and D. Brancazio, "CAD-Casting: Direct Fabrication of Ceramic Shells and Cores by Three-Dimensional Printing," *Manuf. Rev. (USA),* **5** [2] 117-26 (1992).

6. J. D. Yates and S. J. Lombard, "Strain Mismatch and Deformation of Slip Cast Alumina Bodies: The Effects of Solids Loading, Dispersant Concentration, and Binder Concentration"; pp. 1-14, Vol. 23, *Materials & Equipment/Whitewares: Ceramic Engineering and Science Proceedings.* Edited by W. M. Carty. John Wiley & Sons, Inc., Westerville, OH, 2002.

7. K. A. Appiagyei, G. L. Messing, and J. Q. Dumm, "Aqueous Slip Casting of Transparent Yttrium Aluminum Garnet (YAG) Ceramics," *Ceram. Int.,* **34** [5] 1309-13 (2008).

8. M. Boaro, J. M. Vohs, and R. J. Gorte, "Synthesis of Highly Porous Yttria-Stabilized Zirconia by Tape-Casting Methods," *J. Am. Ceram. Soc.*, **86** [3] 395-400 (2003).

9. X. J. Mao, S. Shimai, M. J. Dong, and S. W. Wang, "Gelcasting and Pressureless Sintering of Translucent Alumina Ceramics," *J. Am. Ceram. Soc.*, **91** [5] 1700-2 (2008).

10. R. E. Mistler, D. J. Shanefield, R. B. Runk, "Tape Casting of Ceramics"; pp. 411-48, Ceramic Processing before Firing. Edited by G. Y. Onoda, Jr. and L. L. Hench. John Wiley & Sons, Inc. NY, USA, 1978.

11. R. Moreno, "The Role of Slip Additives in Tape-Casting Technology. I: Solvents and Dispersants," *Am. Ceram. Soc. Bull.,* **71** [10] 1521-31 (1992).

12. T. P. Hyatt, "Electronics: Tape Casting, Roll Compaction," *Am. Ceram. Soc. Bull.,* **74** [10] 56-9 (1995).

13. K. R. Mikeska and W. Cannon, "Non-Aqueous Dispersion Properties of Pure Barium Titanate for Tape Casting," *Colloids Surf.,* **29** [3] 305-21 (1988).

14. D. Saha, R. Giri, K. K. Mistry, and K. Sengupta, "Magnesium Chromate–TiO_2 Spinel Tape Cast Thick Film as Humidity Sensor," *Sens. Actuators B: Chemical,* **107** [1] 323-31 (2005).

15. M. Wagner, A. Roosen, H. Oostra, R. Höppener, and M. De Moya, "Novel Low Voltage Piezoactuators for High Displacements," *J. Electroceram.,* **14** [3] 231-8 (2005).

16. X. W. Ba, J. Li, Y. B. Pan, Y. P. Zeng, H. M. Kou, W. B. Liu, J. Liu, L. X. Wu, and J. K. Guo, "Comparison of Aqueous-and Non-Aqueous-Based Tape Casting for Preparing YAG Transparent Ceramics," *J. Alloys Compd.,* **577** 228-31 (2013).

17. B. M. Schulz, M. T. Brumbach, C. M. Caughel, and W. M. Carty, "Adsorption of Poly(Acrylic Acid) on Clay Surfaces, the Effects of Washing to Remove Impurity Species Present in the Clay"; pp. 149-75, Vol. 24, *Whitewares and Materials: Ceramic Engineering and Science Proceedings.* Edited by W. M. Carty. John Wiley & Sons, Inc., Westerville, OH, 2003.

18. A. Degen and M. Kosec, "Effect of pH and Impurities on the Surface Charge of Zinc Oxide in Aqueous Solution," *J. Eur. Ceram. Soc.,* **20** [6] 667-73 (2000).

19. S. B. Reddy, P. P. Singh, N. Raghu, and V. Kumar, "Effect of Type of Solvent and Dispersant on Nano PZT Powder Dispersion for Tape Casting Slurry," *J. Mater. Sci.,* **37** [5] 929-34 (2002).

20. B. R. Sundlof and W. M. Carty, "Organic and Inorganic Dispersion of Alumina"; pp. 151-66, Vol. 20, *Materials & Equipment/Whitewares: Ceramic Engineering and Science Proceedings.* Edited by W. M. Carty. John Wiley & Sons, Inc., Westerville, OH, 1999.

21. W. M. Carty, "Rheology and Plasticity for Ceramic Processing"; pp. 29-52, Vol. 125, *Fundamentals of Refractory Technology.* Edited by J.P. Bennett, J.D. Smith. John Wiley & Sons, Inc., Westerville, OH, 1999.

22. O. O. Omatete, M. A. Janney, and R. A. Strehlow, "Gelcasting: a New Ceramic Forming Process," *Am. Ceram. Soc. Bull.* **70** (10) 1641-9 (1991).

23. M. A. Janney and O. O. Omatete, "Method for Molding Ceramic Powders Using a Water-based Gel Casting," U.S. Pat. 5,028,362A, July, 1991.

24. A. C. Young, O. O. Omatete, M. A. Janney, and P. A. Menchhofer, "Gelcasting of Alumina," *J. Am. Ceram. Soc.,* **74** [3] 612-8 (1991).

25. S. L. Morissette and J. A. Lewis, "Chemorheology of Aqueous-Based Alumina-Poly (Vinyl Alcohol) Gelcasting Suspensions," *J. Am. Ceram. Soc.,* **82** [3] 521-8 (1999).

26. J. K. Montgomery, P. L. Drzal, K. R. Shull, and K. Faber, "Thermoreversible Gelcasting: a Novel Ceramic Processing Technique," *J. Am. Ceram. Soc.*, **85** [5] 1164-8 (2002).

27. E. Adolfsson, "Gelcasting of Zirconia Using Agarose," *J. Am. Ceram. Soc.,* **89** [6] 1897-902 (2006).

28. J. W. Halloran, V. Tomeckova, S. Gentry, S. Das, P. Cilino, D. Yuan, R. Guo, A. Rudraraju, P. Shao, T. Wu, T. R. Alabi, W. Baker, D. Legdzina, D. Wolski, W. R. Zimbeck, and D. Long, "Photopolymerization of Powder Suspensions for Shaping Ceramics," *J. Eur. Ceram. Soc.,* **31** [14] 2613-9 (2011).

29. M. Takeshita and S. Kurita, "Development of Self-hardening Slip Casting," *J. Eur. Ceram. Soc.,* **17** [2] 415-9 (1997).

30. X. J. Mao, S. Shimai, M. J. Dong, and S. W. Wang, "Gelcasting of Alumina Using Epoxy Resin as a Gelling Agent," *J. Am. Ceram. Soc.,* **90** [3] 986-8 (2007).

31. J. F. Xue, M. J. Dong, J. Li, G. H. Zhou, and S. W. Wang, "Gelcasting of Aluminum Nitride Ceramics," *J. Am. Ceram. Soc.,* **93** [4] 928-30 (2010).

32. X. J. Mao, S. Shimai, and S. W. Wang, "Gelcasting of Alumina Foams Consolidated by Epoxy Resin," *J. Eur. Ceram. Soc.,* **28** [1] 217-22 (2008).

33. Y. Yang, S. Shimai, and S. W. Wang, "Room-Temperature Gelcasting of Alumina with a Water-Soluble Copolymer," *J. Mater. Res.*, **28** [11] 1512-6 (2013).

34. Y. Yang, S. Shimai, Y. Sun, M. J. Dong, H. Kamiya, and S. W. Wang, "Fabrication of Porous Al_2O_3 Ceramics by Rapid Gelation and Mechanical Foaming," *J. Mater. Res.,* **28** [15] 2012-6 (2013).

35. S. Shimai, Y. Yang, S. W. Wang, and H. Kamiya, "Spontaneous Gelcasting of Translucent Alumina Ceramics," *Opti. Mater. Express,* **3** [8] 1000-6 (2013).

36. X. Shu, J. Li, H. L. Zhang, M. J. Dong, S. Shunzo, and S. W. Wang, "Gelcasting of Aluminum Nitride Using a Water-Soluble Copolymer," *J. Inorg Mater.,* **29** [3] 327-30 (2014).

37. Y. Sun, S. Shimai, X. Peng, G. H. Zhou, H. Kamiya, and S. W. Wang, "Fabrication of Transparent Y_2O_3 Ceramics Via Aqueous Gelcasting," *Ceram. Int.,* **40** [6] 8841-5 (2014).

38. Y. Sun, S. Shimai, X. Peng, M. J. Dong, H. Kamiya, and S. W. Wang, "A Method for Gelcasting High-Strength Alumina Ceramics with Low Shrinkage," *J. Mater. Res.,* **29** [02] 247-51 (2014).

39. B. Schwartz, "Review of Multilayer Ceramics for Microelectronic Packaging," *J. Phys. Chem. Solids,* **45** [10] 1051-68 (1984).

40. L. C. Sengupta, E. Ngo, M. E. O'Day, S. Stowell, R. Lancto, S. Sengupta and T. V. Hynes, "Electronically Graded Multilayer Ferroelectric Composites," U.S. Pat. 5,693,429A, December, 1997.

41. T. Chartier and A. Bruneau, "Aqueous Tape Casting of Alumina Substrates," *J. Eur. Ceram. Soc.,* **12** [4] 243-7 (1993).

42. S. C. Singhal, "Solid Oxide Fuel Cells for Stationary, Mobile, and Military Applications," *Solid State Ionics,* **152** 405-10 (2002).

43. G. De Portu, L. Micele, and G. Pezzotti, "Laminated Ceramic Structures from Oxide Systems," *Composites Part B,* **37** [6] 556-67 (2006).

44. G. N. Howatt, R. G. Breckenridge, and J. M. Brownlow, "Fabrication of Thin Ceramic Sheets for Capacitors," *J. Am. Ceram. Soc.,* **30** [8] 237-42 (1947).

45. K. R. Mikeska and W. R. Cannon, "Non-Aqueous Dispersion Properties of Pure Barium Titanate for Tape Casting," *Colloids Surf.,* **29** [3] 305-21 (1988).

46. E. Antolini, M. Ferretti, and S. Gemme, "Preparation of Porous Nickel Electrodes for Molten Carbonate Fuel Cells by Non-Aqueous Tape Casting," *J. Mater. Sci.,* **31** [8] 2187-92 (1996).

47. A. Ceylan, E. Suvaci, and H. Mandal, "Role of Organic Additives on Non-Aqueous Tape Casting of Sialon Ceramics," *J. Eur. Ceram. Soc.,* **31** [1] 167-73 (2011).

48. Y. J. Qiao, Y. Y. Liu, A. D. Liu, and Y. Wang, "Boron Carbide Green Sheet Processed by Environmental Friendly Non-Aqueous Tape Casting," *Ceram. Int.*, **38** [3] 2319-24 (2012).

49. N. Ushifusa and M. J. Cima, "Aqueous Processing of Mullite-Containing Green Sheets," *J. Am. Ceram. Soc.,* **74** [10] 2443-7 (1991).

50. D. Hotza and P. Greil, "Review: Aqueous Tape Casting of Ceramic Powders," *Mater. Sci. Eng., A,* **202** [1] 206-17 (1995).

51. M. P. Albano and L. B. Garrido, "Aqueous Tape Casting of Yttria Stabilized Zirconia," *Mater. Sci. Eng., A,* **420** [1] 171-8 (2006).

52. L. H. Luo, Y. Lang, Z. Z. Huang, L. Cheng, and J. J. Shi, "Fabrication of YSZ Film by Aqueous Tape Casting Using PVA-B1070 Cobinder for IT-SOFC," *Key Eng. Mater.,* **434** 735-8 (2010).

53. C. Pagnoux, T. Chartier, M. de F. Granja, F. Doreau, J. M. Ferreira, and J. F. Baumard, "Aqueous Suspensions for Tape-Casting Based on Acrylic Binders," *J. Eur. Ceram. Soc.,* **18** [3] 241-7 (1998).

54. F. Snijkers, A. De Wilde, S. Mullens, and J. Luyten, "Aqueous Tape Casting of Yttria Stabilised Zirconia Using Natural Product Binder," *J. Eur. Ceram. Soc.,* **24** [6] 1107-10 (2004).

55. M. P. Albano and L. B. Garrido, "Influence of the Slip Composition on the Properties of Tape-Cast Alumina Substrates," *Ceram. Int.,* **31** [1] 57-66 (2005).

56. J. M. LeBeau and Y. Boonyongmaneerat, "Comparison Study of Aqueous Binder Systems for Slurry-Based Processing," *Mater. Sci. Eng., A,* **458** [1] 17-24 (2007).

57. A. Navarro, J. R. Alcock, and R. W. Whatmore, "Aqueous Colloidal Processing and Green Sheet Properties of Lead Zirconate Titanate (PZT) Ceramics Made by Tape Casting," *J. Eur. Ceram. Soc.,* **24** [6] 1073-6 (2004).

58. K. Nagata, "Correlation of Conformation of Acrylic Polymers in Aqueous Suspensions and Properties of Alumina Green Sheets," *Ceram. Trans.,* **26** 205-10 (1991).

59. R. C. Chiu and M. J. Cima, "Drying of Granular Ceramic Films: II, Drying Stress and Saturation Uniformity," *J. Am. Ceram. Soc.,* **76** [11] 2769-77 (1993).

60. J. C. Williams, "Doctor-Blade Process"; pp. 173-98, Vol. 9, *Treatise on Maerial Science and Technology*. Edited by F. Y. Wang, Academic Press, New York, 1976.

61. M. Kemr and H. Mizuhara. “Flexible Ceramic Tape And Method of Making Same,” U.S. Pat. 4,329,271A, May, 1982.

62. K. Kita, J. Fukuda, H. Ohmura, and T. Sakai. “Ceramic Ceramic Tapes and Method of Producing Them,” U.S. Pat. 4,353,956A, October 1982.

63. J. E. Schuetz, I. A. Khoury, and R. Dichiara, "Water-Based Binder for Tape Casting," *Ceram. Ind.,* **129** [5] 42 (1987).

64. N. R. Gurak, P. Josty, and R. Thompson, "Properties and Uses of Synthetic Emulsion Polymers as Binders in Advanced Ceramics Processing," *Am. Ceram. Soc. Bull.,* **66** [10] 1495-7 (1987).

65. P. Nahass, W. E. Rhine, R. L. Pober, H. K. Bowen, and W. L. Robbins, "A Comparison of Aqueous and Nonaqueous Slurries for Tape-Casting, and Dimensional Stability in Green Tapes"; pp. 355-64, Vol. 15. Materials and processes in Microelectronic systems, Ceramic Tranactions. Edited by K. M. Nair, R. Pohanka, and R. C. Buchanan, American Ceramic Society, Westerville, OH, 1990.

66. P. Nahass, R. L. Pober, W. E. Rhine, W. L. Robbins, and H. K. Bowen, "Prediction and Explanation of Aging Shrinkage in Tape-Cast Ceramic Green Sheets," *J. Am. Ceram. Soc.,* **75** [9] 2373-8 (1992).

67. K. Nagata, "Dynamic Viscoelastic Measurements of Suspension for the Drying Process in Tape Casting," *J. Ceram. Soc. Japan,* **100** [11] 1352-6 (1992).

68. K. Nagata, "Rheological Behaviour of Suspension and Properties of Green Sheet: Effect of Compatibility between Dispersant and Binder," *J. Ceram. Soc. Japan,* **100** [10] 1271-5 (1992).

69. K. Nagata, "Effect of Functionalities of Binders on Rheological Behavior of Alumina Suspensions and Properties of Green Sheets," *Nippon Seram. Kyo. Gak.,* **101** [8] 845-9 (1993).

70. J. H. Jean, S. F. Yeh, and C. J. Chen, "Adsorption of Poly (Vinyl Butyral) in Non-Aqueous Ferrite Suspensions," *J. Mater. Res.,* **12** [04] 1062-8 (1997).

71. Y. Yang and Y. Q. Wu, "New Gelling Systems to Fabricate Complex-Shaped Transparent Ceramics," *Proc. SPIE,* **8708** 87080(D)1-8, (2013)

72. N. E. Suyatma, L. Tighzert, A. Copinet, and V. Coma, "Effects of Hydrophilic Plasticizers on Mechanical, Thermal, and Surface Properties of Chitosan Films," *J. Agric. Food. Chem.,* **53** [10] 3950-7 (2005).

73. R. A. Terpstra, P. P. A. C. Pex, and A. H. de Vries, *Ceramic Processing*; pp. 147-73. Chapman & Hall, New York, London, 1995.

74. D. J. Bucher, V. J. Harriott, and L. G. Roberts, "Skeletal Micro-Density, Porosity and Bulk Density of Acroporid Corals," *J. Exp. Mar. Biol. Ecol.,* **228** [1] 117-36 (1998).

75. B. J. Briscoe, G. Lo Biundo, and N. Özkan, "Drying Kinetics of Water-Based Ceramic Suspensions for Tape Casting," *Ceram. Int.,* **24** [5] 347-57 (1998).

76. G. S. Grader and L. Zuri, "Tape Casting Slip Preparation by in Situ Polymerization," *J. Am. Ceram. Soc.,* **76** [7] 1809-14 (1993).

77. A. Kristoffersson and E. Carlström, "Tape Casting of Alumina in Water with an Acrylic Latex Binder," *J. Eur. Ceram. Soc.,* **17** [2] 289-97 (1997).

78. Y. P. Zeng, D. L. Jiang, and P. Greil, "Tape Casting of Aqueous Al_2O_3 Slurries," *J. Eur. Ceram. Soc.,* **20** [11] 1691-7 (2000).

79. B. Bitterlich, C. Lutz, and A. Roosen, "Rheological Characterization of Water-Based Slurries for the Tape Casting Process," *Ceram. Int.,* **28** [6] 675-83 (2002).

80. T. J. Soltesz, W. M. Carty, H. J. Miller, T. R. Armstrong, and P. Smith, "Rheological Process Control Diagram for Tape Casting," *Ceram. Trans,* **88** 391-402 (1997).

81. A. Kristoffersson, E. Roncari, and C. Galassi, "Comparison of Different Binders for Water-Based Tape Casting of Alumina," *J. Eur. Ceram. Soc.,* **18** [14] 2123-31 (1998).

82. R. W. Wenig and G. L. Schrader, "In Situ FTIR(Fourier Transform IR) Spectroscopy of 1-Butene and 1,3-Butadiene. Selective Oxidation to Maleic Anhydride on Vanadium-Phosphorus-Oxygen Catalysts," *J. Phys. Chem.,* **91** [7] 1911-8 (1987).

83. M. N. Rahaman, *Ceramic Processing*; pp. 141-91. Taylor & Francis Group, Boca Raton, FL, 2006.

84. K. M. Kinsman, J. McKittrick, E. Sluzky, and K. Hesse, "Phase Development and Luminescence in Chromium-Doped Yttrium Aluminum Garnet (YAG: Cr) Phosphors," *J. Am. Ceram. Soc.,* **77** [11] 2866-72 (1994).